The indoor environment - a potential source for intact human-associated anaerobes

Manuela-Raluca Pausan[1,#,±], Marcus Blohs[1,±], Alexander Mahnert[1], Christine Moissl-Eichinger[1,*]

[1] Diagnostic and Research Institute of Hygiene, Microbiology and Environmental Medicine, Medical University of Graz, Graz 8010, Austria

[±] Authors contributed equally

*Corresponding author

[#] Current affiliation: Steigerwald Arzneimittelwerk GmbH, Bayer Consumer Health, Havelstrasse 5, D-64295 Darmstadt, Germany

Abstract

Background. People in westernised countries spend most of their time indoors. A healthy human microbiome relies on the interaction with and exchange of microbes that takes place between the human body and its environment. For this reason, the built environment might represent a potent source of commensal microbes. Anaerobic microbes are of particular interest, as researchers have not yet sufficiently clarified how the human microbiome acquires oxygen-sensitive microbes, such as obligate or facultative anaerobes.

Methods. We sampled ten households and used propidium monoazide to assess the viability of the collected prokaryotes. We compared the microbiome profiles based on 16S rRNA gene sequencing and confirmed our results by genetic and cultivation-based analyses.

Results. Quantitative and qualitative analysis revealed that most of the microbial taxa are of human origin. Less than 25% of the prokaryotic signatures found in built environment (BE) samples originate from intact – and thus potentially living – cells, indicating that aerobic and stress resistant taxa display an apparent survival advantage. Although the dominant microbial fraction identified on the bathroom floors is composed of aerobes, we confirmed the presence of strictly anaerobic taxa, including methanogenic archaea, in PMA-treated samples. As methanogens are regarded as highly sensitive to aerobic conditions, oxygen-tolerance experiments were performed with human-associated isolates to validate their survival. These results show that these taxa have a limited but substantial ability to survive in the BE. We determined that human-associated methanogens can survive oxic conditions for at least 6 h.

Conclusions. This study enabled us to collect strong evidence that supports the hypothesis that obligate anaerobic taxa can survive in the BE for a limited amount of time. This suggests that the BE serves as a potential source of anaerobic human commensals.

Background

The development of a healthy human microbiome depends on extensive microbial transmission from other hosts, food, water, but also reservoirs in the built environment (BE; Browne et al., 2017). Especially for newborn infants, the acquisition of microbes is a crucial process, as they represent an empty niche for a variety of microorganisms. In this way, they differ from adults, who usually have well-established, complex and stable microbiomes. A fairly stable microbiome is normally achieved by the third year after birth [2] and, up until this point, numerous microorganisms are acquired from other microbiomes. Various factors affect this maturation process, including its speed and quality. These factors include the birth mode (Caesarean section vs. vaginal birth), type of feeding (breast-fed vs. formula-fed), medication (e.g. antibiotics), time point of introduction of solid food, quality of social interactions and contact to animals and nature [3–6]. During the maturation of the intestinal microbiome, facultative anaerobic microorganisms, which initially thrive in the gastrointestinal tract (GIT) after birth, are subsequently replaced by obligate anaerobes. The latter support the optimal fermentation of solid food [7,8].

The abiotic BE together with its indoor microbiome (reviewed by Chase et al., 2016; Karen C. Dannemiller, 2019; Gilbert & Stephens, 2018; Horve et al., 2020; Kelley & Gilbert, 2013) is considered to have an important role in the development and maintenance of a healthy human microbiome [1]. Populations in urban areas of high-income countries currently spend on average 90% of the day indoors; therefore, the abiotic BE and its indoor microbiome represent one of the major reservoirs of environmental microbes [14]. This reservoir plays a vital role in feeding and shaping the human microbiome early in life (see A. W. Brooks et al., 2018; B. Brooks et al., 2014), but it also likely contributes to recolonisation after disease and infection or antibiotic treatment [17,18].

Cross-talk between the human being and the BE can have both positive and negative aspects. On the one hand, indoor microbes could trigger immediate health issues under rare circumstances. This aspect is of particular concern in the course of pathogen and resistance transmission in hospital environments [19–21]. On the other hand, several studies have pointed out the beneficial effects of a healthy indoor microbiome and presented the observation that the presence of animal-associated and farm-like indoor microorganisms in rural areas is linked to decreased asthma and allergy risk [22–24].

For microbes to be transmitted successfully between hosts via the built environment, they have to be able to survive outside of their natural habitat (“ex-host” survivability) [1,25]. The majority of human commensals are subject to a number of different stressors, including UV radiation, adverse temperature and desiccation [1]. For gut commensals, the exposure to atmospheric oxygen is a critical factor, as an estimated 99% of all microorganisms that thrive in the distal colon are obligate anaerobes [26]. The extent of aero-tolerance among species varies, and strictly anaerobic taxa are usually unable to actively replicate outside of the gastrointestinal tract (GIT; Ley et al., 2008; Meehan & Beiko, 2014). To overcome this limitation, numerous (anaerobic) bacteria protect themselves through sporulation, as this provides them with the opportunity to escape difficult environmental situations for an extended period of time. It is estimated that about 30% of the genera in the total intestinal microbiota are capable of spore-formation, including *Lachnospiraceae*, *Ruminococcaceae*, *Clostridiaceae* and *Peptostreptococcaceae* [29]. After being transferred to their new environment, spores react to trigger signals (such as bile acids) by germinating, spreading and colonising in the new host thereafter [29].

Non-spore formers, however, must have other strategies that allow them to tolerate environmental stress factors. Strictly anaerobic microorganisms such as *Roseburia* usually die within few minutes of exposure to atmospheric oxygen, as they have not evolved mechanisms that enable them to avoid and repair the damage caused by reactive oxygen species (ROS); i.e. they lack catalases, peroxidases, or superoxide dismutases [30,31]. Thus,

the survival strategies and transmission routes of most of the strictly anaerobic microbiome members, including methanogenic archaea, are largely unknown.

Methanogenic archaea ("methanogens") represent important components of the human GIT, along with bacteria, viruses and small eukaryotes [32]. These archaea are obligate anaerobic microorganisms and lack the ability to form spores. Despite their oxygen sensitivity, the most common representative, *Methanobrevibacter smithii*, can be detected in almost 96% of the adult population [33]. Interestingly, *M. smithii* is rarely found in younger cohorts [34], and especially uncommon in children born via Caesarean section [35].

In this communication, we address a major question: Can the BE be a potential reservoir for anaerobic, commensal microorganisms? To answer this question, we analysed the indoor microbiome of ten households and compared the microbiome data with the human microbiome data. As the bathroom represents a rich source of GIT-derived microorganisms [36–38], we sampled surfaces near toilets in different households. One major shortcoming of previous studies was that no distinction was made between viable microorganisms (i.e. those with the potential to colonise a new host) and non-viable microorganisms [1]. We addressed this knowledge gap by combining a propidium monoazide (PMA) treatment with high-throughput 16S rRNA gene sequencing. This procedure enabled us to identify the signatures of intact, and thus probably living, microorganisms. As archaeal cells were frequently detected amongst the surviving proportion of the BE microbiome, we analysed the BE archaeome in more detail. The results of this analysis show that human-associated methanogens can survive air exposure and, therefore, could be transferred to another human microbiome through the BE.

Material and methods

Sample collection and DNA extraction

Samples were collected from ten different family houses in the vicinity of Graz, Austria (in March 2017). All houses were occupied by at least one adult and five of the houses by families with children. The sampling surface was selected by considering the richest source of GIT-derived microorganisms [36], namely the bathroom. Per household, two areas of 30 cm^2 in the proximity of the toilet (example shown in Supplementary Fig. 1a) were cleaned with bleach and sterile water and left uncovered and untouched for 7 days. After 7 days, the areas were sampled using a sterile nylon swab (FLOQSwabsTM, Copan, Brescia, Italy) that has been dipped in 0.9% saline (NaCl) solution. Each area was sampled with the swab three times, by rotating the swab every time before sampling the area again (Supplementary Fig. 1b). Metadata collected from the households can be found in Supplementary Table 1. One swab was opened, exposed to the air in an indoor environment and used as a negative control. Additionally, extraction blank controls were added during the DNA extraction step and PCR to identify possible microbial contaminants in the reagents.

The samples were transported back to the laboratory on ice packs on the day of the sampling. One of the two samples from each house, which were collected in parallel, was treated with PMA (Biotium, Inc., Hayward, CA) based on manufacturer´s recommendations and as previously described [39] to differentiate between cells with an intact membrane. Briefly, swabs were transferred to DNA-free 0.9% NaCl-solution and PMA was added to a final concentration of 50 µM and incubated for 5 min on a shaker in the dark. Photoactivation of PMA was performed for 15 min using the PMA-lite™ LED Photolysis device including an intermediate mixing step. PMA is a photo-reactive DNA binding dye which intercalates with free DNA inhibiting downstream DNA amplification thereof. As PMA is not permeable for intact cell walls, a molecular distinction between PMA-masked free DNA from disrupted, most

136 probably dead cells, and DNA from intact, most probably living cells can be made [40]. In the
137 following, we use the term “PMA” to indicate samples treated with PMA (= intact cells only),
138 and the term “non-PMA” for samples not treated with PMA (= both, intact and dead cells/free
139 DNA).

140 For genomic DNA extraction, the indoor samples were processed using the FastDNA Spin Kit
141 (MP Biomedicals, Germany) according to manufacturer's instructions. The genomic DNA was
142 eluted in 100 µL elution buffer, and the concentration was measured using Qubit™ dsDNA HS
143 Assay Kit (ThermoFisher Scientific).

144

145 **PCR and qPCR**

146 The obtained genomic DNA was used to amplify the V4 region of the 16S rRNA gene using
147 Illumina-tagged primers 515F and 806R (Supplementary Tab. 2). In order to identify the
148 archaeal communities present in the samples, a nested PCR was performed using the primer
149 combination 344F-1041R/Illu519F-Illu806R as described previously [41]. The PCR reaction
150 was performed in a final volume of 25 µL containing: TAKARA Ex Taq® buffer with $MgCl_2$ (10
151 X; Takara Bio Inc., Tokyo, Japan), primers 200 nM, dNTP mix 200 µM, TAKARA Ex Taq®
152 Polymerase 0.5 U, water (Lichrosolv®; Merck, Darmstadt, Germany), and DNA template (1-2
153 µL of genomic DNA). The PCR amplification conditions are listed in Supplementary Tab. 3.

154 The bacterial and archaeal 16S rRNA gene copies were determined using SYBR based
155 quantitative PCR (qPCR) with the primer pair Bac331F-Bac797R and A806f-A958r,
156 respectively (Supplementary Tab. 2). The reaction mix contained: 1x SsoAdvanced™
157 Universal SYBR® Green Supermix (Bio-Rad, Hercules, USA), 300 nM of forward and reverse
158 primer, 1 µL gDNA template, PCR grade water (Lichrosolv®; Merck, Darmstadt, Germany).
159 The qPCR was performed in triplicates using the CFX96 Touch™ Real-Time PCR Detection
160 System (Bio-Rad, Hercules, USA). The qPCR conditions are given in Supplementary Tab. 3.

Crossing point (Cp) values were determined using the regression method within the Bio-Rad CFX Manager software version 3.1. Absolute copy numbers of bacterial 16S rRNA genes were calculated using the Cp values and the reaction efficiencies based on standard curves obtained from defined DNA samples from *Escherichia coli* and *Nitrososphaera viennensis* [42]. The qPCR efficiency was between 85-105%, and the R^2 values were always above 0.9. Detection limits were defined based on the average Cp values of non-template controls (triplicates) and the corresponding standard curves of the positive controls.

NGS-based 16S rRNA gene sequencing

Library preparation and sequencing of the amplicons were carried out at the Core Facility Molecular Biology, Center for Medical Research at the Medical University Graz, Austria. In brief, DNA concentrations were normalised using a SequalPrep™ normalisation plate (Invitrogen), and each sample was indexed with a unique barcode sequence (8 cycles index PCR). After pooling of the indexed samples, a gel cut was carried out to purify the products of the index PCR. Sequencing was performed using the Illumina MiSeq device and MS-102-3003 MiSeq® Reagent Kit v3-600cycles (2x150 cycles). The obtained fastq data is available in the European Nucleotide Archive under the study accession number: PRJEB41618.

The fastq data analysis was performed using QIIME2 [43] as described previously [44]. After quality filtering, the DADA2 algorithm [45] was used to denoise truncated reads and generate amplicon sequence variants (ASVs). Taxonomic classification [46] was based on the SILVA v132 database [47] and the obtained feature table and taxonomy file were used for further analysis (Supplementary Tab. 4). The overlapping features from negative controls (DNA extraction and PCR negative controls) were manually subtracted or removed from both the bacterial and archaeal dataset. The reads classified as chloroplast and mitochondria were also removed.

Human microbiome data

In order to assess to which extent the microbial community indoors is affected and affects the human microbiome, a representative dataset of the human microbiome from several body sites was collected. We took advantage of several previous in-house projects, covering the microbiome of skin, nasal cavity, saliva, urine, vagina, and stool (for more details, please see: Supplementary Tab. 5). All samples were taken from healthy participants and processed in our lab with methods similarly to the current study: DNA was extracted by a combination of enzymatic and mechanical lysis; amplification of the 16S rRNA gene was done using the "universal" primers based on Caporaso et al. (2011) [48] or the slightly adapted primers according to Walters et al. (2016) [49]. Library preparation, as well as sequencing, were performed by the Core Facility Molecular Biology at the Medical University Graz, Austria. Obtained raw reads were processed in parallel to the indoor microbiome data of the current study (Supplementary Tab. 6 and 9).

Data analysis and statistics

In general, data analysis of the microbial data is based on the indoor data alone (Supplementary Tab. 4 and 9). Comparative analysis between indoor and human microbiomes are based on the mixed dataset (Supplementary Tab. 6 and 10). Bar charts, box plots, and bubble plots are based on relative abundances and were constructed for both the bacterial and archaeal communities at different taxonomic levels using the *phyloseq* [50] and *ggplot2* package in R [51]. Significant differences between microbial taxa were calculated in R using Wilcoxon signed-rank tests for dependent samples (e.g. PMA and non-PMA) or Mann–Whitney *U* test for independent samples (e.g. indoor and human). P values were adjusted for multiple testing using the method after Benjamini & Hochberg (1995). The online-tool Calypso [53] was used to calculate alpha diversity metrics, Linear discriminant analysis Effect Size (LEfSe), the bar plots and principal coordinates analysis (PCoA) plots based on Bray-Curtis. Before analysis in Calypso, the data was normalised using total sum normalisation (TSS)

combined with square root transformation. For alpha diversity, reads were rarefied to 5,588 and analysed based on Shannon and richness indices. To test for differences in the beta diversity between sample categories, PERMANOVA analysis was performed in QIIME2 based on Bray-Curtis distances. BugBase [54] was used to predict potential phenotypes such as aerobic, anaerobic, facultative anaerobic and stress-tolerant communities which were present in the PMA and non-PMA treated samples. SourceTracker2 analysis [55] was performed with default settings. Sampling depth was set to 1,000 reads for source and sink, respectively.

A phylogenetic tree was constructed to determine if the sequences belonging to methanogens identified in the analysed samples are of human origin. All sequences classified within the genera *Methanobacterium*, *Methanobrevibacter* and *Methanomassiliicoccus* from our analysed samples were used for creating the phylogenetic tree. Additionally, 16S rRNA gene sequences of species of *Methanobacterium*, *Methanobrevibacter* and *Methanomassiliicoccus* previously identified in the human body or the environment were included from NCBI and two other studies [5,56]. The alignment was performed using the SILVA SINA alignment tool [57]. The sequences were cropped to the same length using BioEdit and used afterwards to construct a tree based on the maximum-likelihood algorithm with a bootstrap value of 1,000 using MEGA7 [58]. The phylogenetic tree was further processed using the online tool iTOL [59].

Definition of obligate anaerobic taxa

Bacterial and archaeal taxa were annotated as obligate anaerobic on family and genus level and marked with an asterix *. The categorisation is based on the “list of prokaryotes according to their aerotolerant or obligate anaerobic metabolism” V1.3 [60] and literature review.

Cultivation and oxygen tolerance test

An oxygen sensitivity test was implemented to determine if methanogenic archaeal strains can survive under aerobic conditions for a certain period of time. Three human-associated

methanogenic strains (*Methanosphaera stadtmanae* DSM no. 3091, *Methanobrevibacter smithii* DSM no. 2375, and *Methanomassiliicoccus luminyensis* DSM no. 25720) and a newly isolated strain (*Methanobrevibacter* sp., unpublished) have been tested for their ability to survive under aerobic conditions. The human-associated methanogen cultures were obtained from DSMZ and both, *M. stadtmanae* and *M. luminyensis* were grown in MPT1 medium at 37 °C (Mauerhofer et al., unpublished). The new *Methanobrevibacter* strain was isolated in our lab from a fresh stool sample using ATCC medium: 1340 MS medium for methanogens (https://www.atcc.org/). Both *Methanobrevibacter* strains were grown in MS medium at 37°C.

Cultures were used after 3-7 days of growth as follows: 1 mL culture was transferred to sterile 1.5 mL Eppendorf tubes in the anaerobic chamber and centrifuged at 10,000 x g for 10 min, the cell pellet was washed twice either anaerobically for the controls (anaerobically exposed microorganisms) or aerobically for the oxygen exposed microorganisms with 1 mL sterile 1x PBS and centrifuged again at 10,000 x g for 10 min. After removing most of the PBS, the cell pellet was resuspended in the remaining liquid and exposed to aerobic or anaerobic conditions for different time points: 0 h (30 minutes after transfer), 6 h, 24 h, 48 h, and 168 h (7 days). After exposure, the liquid from the tubes was transferred to a sterile growth medium in Hungate tubes in the anaerobic chamber and the cultures were left to grow for 2-3 weeks. Then, the first optical density (OD) measurements (600 nm) and methane measurements were done using a spectrometer and methane sensor (BCP-CH4 sensor, BlueSens). For the methane measurement, 10 mL of gas-phase was taken from the Hungate tubes using an air-tight glass syringe. For each experiment, two sterile unopened Hungate tubes with media served as control, and two inoculated Hungate tubes with 0.5 mL of the culture served as a positive control. In addition, a tube of 1x PBS served as a control for 168h. Each experiment was performed in duplicates. After OD and methane measurements, microscopic observations were performed to determine the shape of the microorganisms growing in the medium. Oxygen saturation of the PBS was monitored in a control experiment using the FireStingO2 optical oxygen meter (PyroScience GmbH) and the oxygen probe OXROB10. Using the

identical methodology as described above we were able to confirm an oxygen saturation in the medium of > 80% at any given time point (0 h, 10 min, 20 min, 30 min, 45 min, 1 h, 2 h, 4 h, 6 h and 24 h) for every strain.

Results

In this section, we present information about the anaerobic microbial communities detected in the bathrooms of the selected family houses. We wanted to determine whether the indoor environment serves as a source of anaerobic, commensal microorganisms, such as methanogens, which could potentially colonise the human body. To achieve this purpose, we collected samples from two surface areas (~30 cm^2) in the bathrooms of ten households.

One of the two samples collected from the BE was treated with PMA in order to mask the DNA of disrupted cells [40]. By comparing non-PMA (untreated) and PMA-treated samples, we could distinguish the overall (non-PMA) microbiome from the intact (i.e. probably alive) microbiome (PMA). This comparison enabled us to draw conclusions regarding the survival of strictly anaerobic microorganisms under exposed conditions. These findings were further supported by the results of subsequent experiments.

Although we present data on all detected microbial signatures, we focused specifically on strictly anaerobic taxa. For convenience, we highlight taxa that mainly consist of strict anaerobes with an asterisk *.

The human microbiome is the predominant source of microbes in the BE

Using a universal 16S rRNA gene sequencing approach, it was possible to obtain overall more than 380,000 sequences (Bacteria: 99.86%, Archaea: 0.14%), corresponding to 3,684 ASVs and an average of 473 ± 110 ASVs per household (285 ± 50 and 245 ± 80 ASVs in non-PMA

and PMA samples, respectively; Supplementary Tab. 4). We observed a high amount of heterogeneity amongst households, with only 26 shared ASVs (0.7%) amongst all households, and 351 ASVs (9.5%) that were shared between at least two households (Supplementary Tab. 7). The 26 ASVs present in all samples include typical skin-associated taxa, such as *Staphylococcus* (11 ASVs) and *Corynebacterium* (8 ASVs), but also *Finegoldia** (6 ASVs) and *Peptoniphilus** (1 ASV).

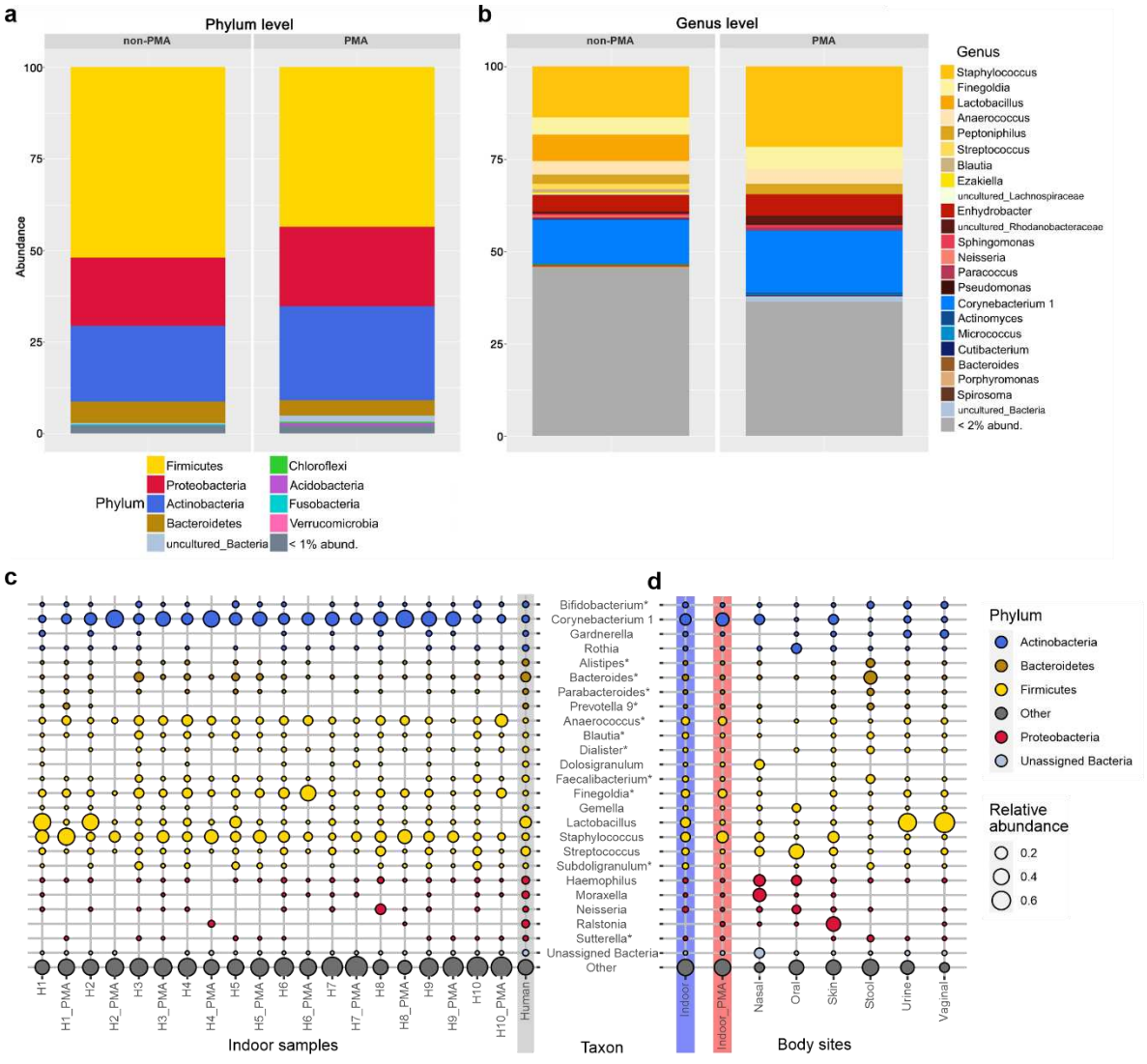

Fig. 1: Distribution and relative abundance of bacterial taxa in samples from different households/bathrooms. Bar charts showing the microbial composition of non-PMA- and PMA-treated bathroom floor samples at the **(a)** phylum and **(b)** genus levels. Genera with < 2% rel. abundance are summarised in grey. Bubble plots display the 25 most abundant genera (bubble size reflects the relative abundance): **(c)** Household samples (H1–H10) are depicted individually for non-PMA and PMA treatment together with human samples (grey background) that represent reads from several body sites: nasal cavity, skin, vagina, urine, stool and oral samples. **(d)** Human samples compared to non-PMA (blue background) and PMA (red background) bathroom samples.

299 Genera are coloured according to their taxonomic phylum, and taxa that predominantly contain strict anaerobes are marked by
300 an asterisk.

301 A total of 32 phyla were observed, and most sequences were classified to four phyla:
302 Firmicutes (52.2% non-PMA, 41.2% PMA), Actinobacteria (20.3% non-PMA, 26.0% PMA),
303 Proteobacteria (18.8% non-PMA, 23.3% PMA) and Bacteroidetes (6% non-PMA, 4.3% PMA)
304 (Fig. 1a). The distribution of sequences classified to these phyla did not change significantly
305 upon PMA treatment. The Linear discriminant analysis Effect Size (LEfSe) method and
306 Wilcoxon signed-rank test were performed, revealing significant differences only in four
307 low-abundance phyla, namely, an increase (Actinobacteria) or decrease (Tenericutes,
308 Fusobacteria, Epsilonbacteraeota) in relative abundance upon PMA treatment ($P < 0.05$,
309 Supplementary Fig. 2).

310 Genera associated with the human skin (e.g. *Staphylococcus, Corynebacterium,*
311 *Streptococcus, Neisseria, Micrococcus, Cutibacterium*), gastrointestinal and genitourinary
312 tract (e.g. *Lactobacillus, Finegoldia*, Bacteroides*, Anaerococcus*, Peptoniphilus**,
313 Lachnospiraceae*) were identified in both non-PMA and PMA samples (Fig. 1c). Notably,
314 *Bifidobacterium*, Rothia, Bacteroides*, Blautia*, Dialister*, Faecalibacterium*, Gemella,*
315 *Subdoligranulum** and *Haemophilus* were detected in every single household, but not in all
316 PMA samples, indicating a potential impairment by environmental stressors.

317 Due to the high proportion of common human-associated commensals, we compared the BE
318 microbiome data collected in this study with human microbiome data that were collected in
319 other studies performed by our lab (see material and methods and Supplementary Tab. 5).
320 The results of a bubble plot analysis of the most abundant genera (Fig. 1d) revealed a specific
321 pattern with respect to the abundance of particular commensals in BE samples or human
322 samples, retrieved from the nasal and oral cavity, skin, stool and vaginal samples. In particular,
323 we observed that signatures of typical human commensals such as *Corynebacterium*,
324 *Anaerococcus**, *Dolosigranulum*, *Finegoldia**, *Gardnerella* and *Staphylococcus* were highly

enriched in non-PMA indoor samples as compared to in human samples ($P_{adj} < 0.001$; Mann–Whitney *U* test), indicating that an efficient transfer to indoor surfaces had occurred.

With respect to alpha diversity, the non-PMA indoor samples showed high Shannon indices, which were comparable to stool samples and even exceeded stool samples in richness by more than two-fold (mean richness is 282 ± 65.3 and 136 ± 30.6 for non-PMA indoor and stool samples, respectively; see Fig. 2). A beta diversity analysis confirmed that all analysed body sites grouped separately ($P_{adj} < 0.01$, PERMANOVA), except for urine and vaginal samples ($P_{adj} = 0.81$; Fig. 2a). However, we did not observe a grouping of indoor samples with a specific human body site, as the clusters differed significantly from one another ($P_{adj} < 0.01$).

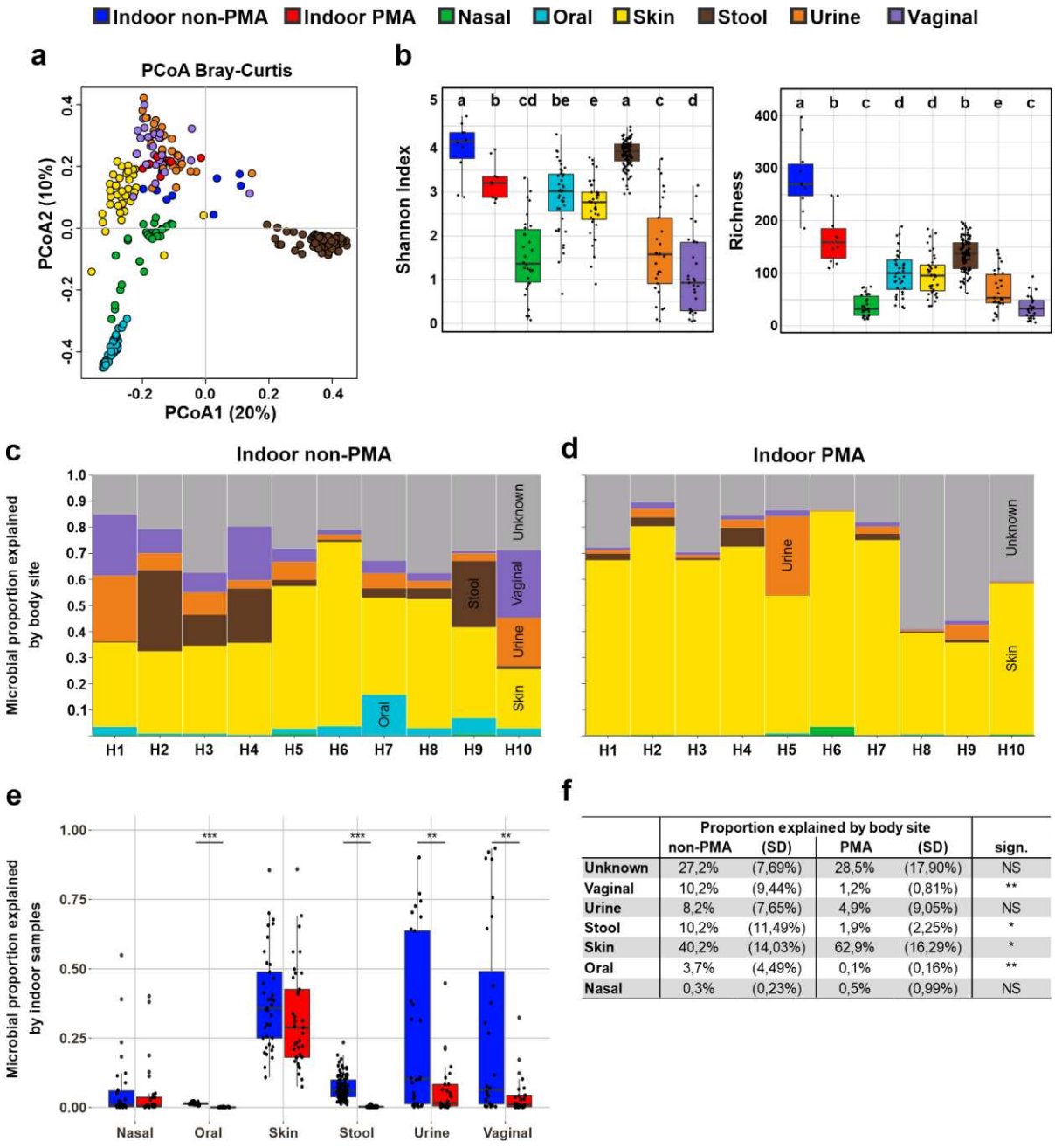

f

	Proportion explained by body site				
	non-PMA	(SD)	PMA	(SD)	sign.
Unknown	27,2%	(7,69%)	28,5%	(17,90%)	NS
Vaginal	10,2%	(9,44%)	1,2%	(0,81%)	**
Urine	8,2%	(7,65%)	4,9%	(9,05%)	NS
Stool	10,2%	(11,49%)	1,9%	(2,25%)	*
Skin	40,2%	(14,03%)	62,9%	(16,29%)	*
Oral	3,7%	(4,49%)	0,1%	(0,16%)	**
Nasal	0,3%	(0,23%)	0,5%	(0,99%)	NS

Fig. 2: A comparison between the indoor and human microbiome. (a) Principal coordinates analysis plots based on Bray-Curtis dissimilarity and **(b)** alpha diversity indices (Shannon, left; richness, right) are depicted for all indoor samples (blue = untreated, red = PMA treated) together with representative human body site samples (green = nasal cavity, light blue = oral, yellow = skin, brown = stool, pink = urine, purple = vaginal). Significant differences are indicated by the different letters above the bars, as defined by a Mann–Whitney *U* test; $P < 0.05$, FDR adjusted (samples that share the same letter do not significantly differ). The proportion of microbes in 10 different bathrooms (H1 – H10) for **(c)** non-PMA and **(d)** PMA samples that can be explained by human body sites or are of unknown origin (grey). Each household is represented by a stacked bar chart, and values were fitted to 100%. **(e)** The proportion of microbes on different body sites that can be potentially explained by the bathroom microbiome; significant differences between treatments were defined by a Kruskal-Wallis test; **, $P < 0.01$; ***, $P < 0.001$. **(f)** The table shows mean values and standard deviations for (d) and (e); significant differences between treatments were defined by performing the Wilcoxon signed-rank test; NS, not significant; *, $P < 0.05$; **, $P < 0.01$.

To determine the level of impact of the human microbiome on our indoor samples, we performed a SourceTracking 2 analysis [55]. Independent of the PMA treatment, about 75% of the indoor microbiome was associated with human sources. These findings indicate that the human body was the dominant source of the microbes detected in bathroom samples (Fig. 3a,b). Nevertheless, depending on the household, we observed large fluctuations in the proportion of human-associated taxa. Especially in PMA samples, this proportion ranges from 41–89%. This may be indicative of a large variation in the frequency and duration of exposure of the tested surfaces to a human being.

Upon PMA treatment, we observed a significant reduction in the vaginal, stool, and oral signatures in the surface samples, while the proportion of microbes from human skin significantly increased ($P < 0.05$, Wilcoxon signed-rank test; see Fig. 3d). These results indicate that skin-related microbes possess the greatest ability to survive in the bathroom environment.

Vice versa, microbial traces from the indoor environment could potentially serve as a source for the human microbiome as well (Fig. 3c). As has been identified in other studies, we identified that the highest level of exchange occurred between human skin and the indoor and human microbes, whereby the skin shared on average 29% and 32% of the microbial signatures with non-PMA and PMA samples from the bathroom. The overlap with other body sites was generally very low, and especially PMA-treated samples shared on average only about 6% of the taxa with urine, 5% with nasal cavity, 4% with vaginal and < 0.01% with oral and stool samples. Therefore, the impact of the bathroom microbiome on human body sites, with the exception of the skin, seems to be very small or even negligible.

Oxygen-tolerance primarily determines microbial survival indoors

Human commensals are exposed to several stress factors in the BE; therefore, many of them are perceived as incapable of surviving in this environment over extended periods. We

performed PMA treatment to mask DNA from disrupted cells, and in fact, the absolute abundance was significantly affected by PMA treatment (Fig. 3a). Results of the quantitative PCR reveal a 4.2-fold decrease in microbial 16S rRNA gene copy number (Fig. 4c), indicating that less than 25% of all microbial signatures originate from intact, probably living cells. This is also reflected by the significant drop in both of the alpha diversity parameters in PMA samples as compared to those in untreated indoor samples (Shannon: $P_{adj} = 0.007$, richness: $P_{adj} = 0.0006$; Wilcoxon rank-sum tests, Fig. 2b). PCoA plots based on Bray-Curtis distances also showed a significant separation based on the PMA treatment ($P_{adj} = 0.018$) even though indoor samples were more similar to one another than to any human body site (Fig. 2a).

LEfSe was performed on PMA and non-PMA samples to determine which taxa are indicative for PMA samples and, therefore, likely to survive in the indoor environment (Supplementary Fig. 3). Representative taxa for PMA were found to be predominantly environmental and aerobic (or aerotolerant) groups, such as *Acidobacteria*, *Micromonosporales*, *Solirubrobacterales*, *Rhizobiales*, *Nocardiaceae*, *Bacillus* and *Sphingomonas,* but also included human skin commensals, such as *Corynebacterium*_1, *Staphylococcus*, or *Rombustia**. On the other hand, representative taxa for non-PMA samples were more diverse in terms of their physiological traits and origins. They predominantly included (facultatively) anaerobic, non-spore forming, human-associated groups, such as *Bacteroidales**, *Lactobacillaceae*, multiple genera in the families *Lachnospiraceae** and *Ruminococcaceae**, *Bifidobacteriaceae**, as well as in *Christensenellaceae**, *Veillonellaceae**, *Haemophilus*, *Neisseria* and the *Eubacterium coprostanoligenes* group*. Interestingly, some opportunistic pathogens (*Atopobium*, *Rothia* and *Campylobacter*) were also characteristic for and significantly enriched in the non-PMA samples (Supplementary Fig. 4), which suggests that these taxa might not survive on BE surfaces over extended periods of time.

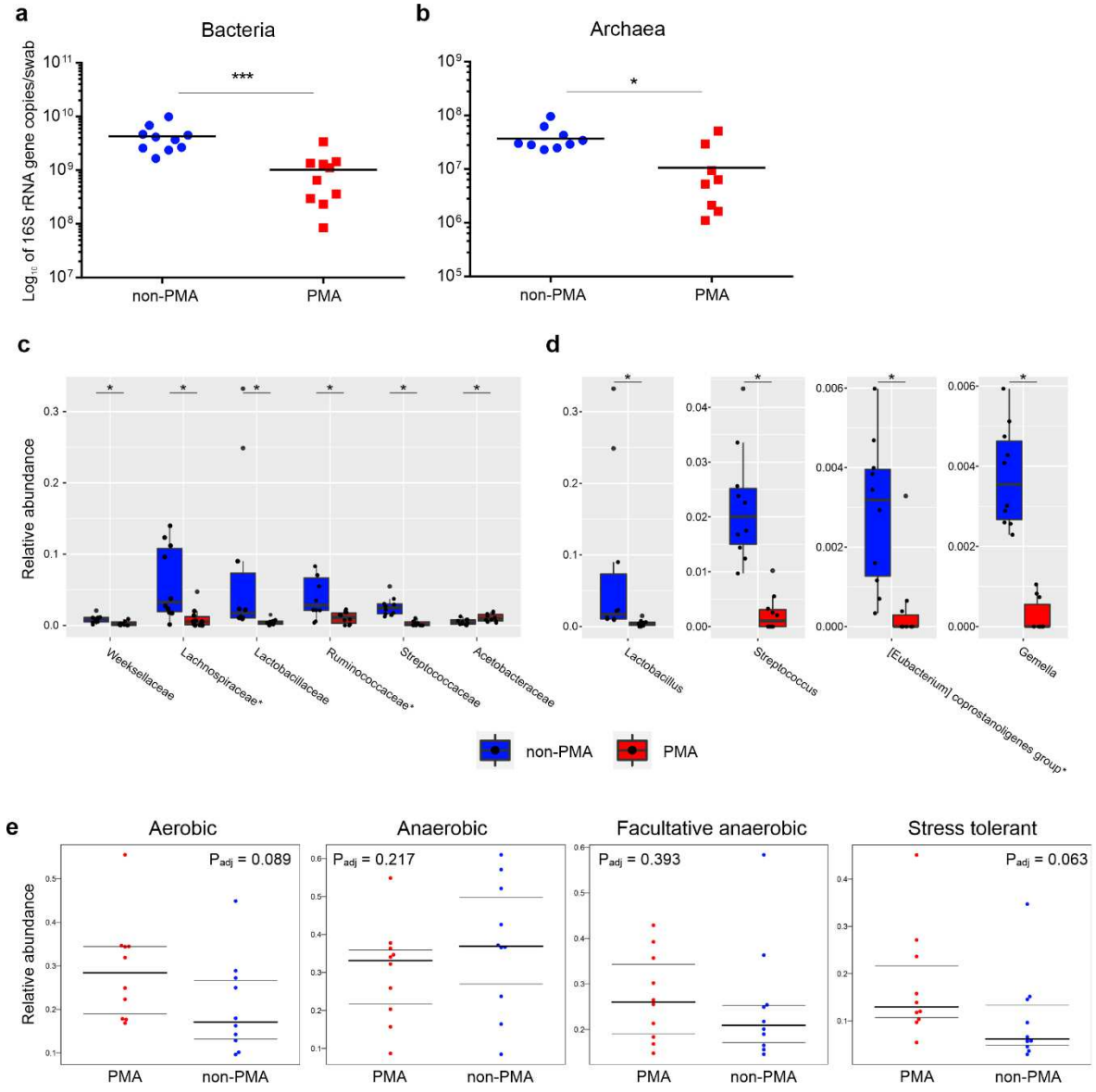

Fig. 3 The effects of PMA treatment on prokaryotic abundance and composition. Quantitative PCR analysis of untreated and PMA-treated bathroom floor samples using **(a)** universal and **(b)** archaeal primer pairs. Wilcoxon signed-rank test analysis results, revealing the relative abundance of the 50 and 100 most abundant bacterial **(d)** families and **(e)** genera, respectively, that were significantly affected by PMA treatment. Strict anaerobic taxa are marked by an asterix. Sign.: FDR-adjusted Wilcoxon signed-rank test; *, $P_{adj} < 0.05$; ***, $P_{adj} < 0.01$. **(e)** The relative abundance of different phenotypes as determined through BugBase. Significances were automatically defined by Mann-Whitney *U* test in BugBase.

After PMA treatment, we observed a significant change in the relative abundance of 53 taxa among the most abundant bacterial genera and families ($P < 0.05$, $n_{genus} = 100$, $n_{family} = 50$, Wilcoxon signed-rank test, Supplementary Tab. 8), although only 10 taxa remained significant after performing an adjustment for multiple testing ($P_{adj} < 0.05$, Fig. 3b,c). In accordance with our LEfSe analysis results, we observed a strong reduction of signals originating from non-

spore forming, (facultative) anaerobic human commensals, and particularly for *Lactobacillus*, *Streptococcus*, *Gemella* and the *Eubacterium coprostanoligenes* group*. *Ruminococcaceae* and several genera within this family also showed a strong reduction in relative abundance upon PMA-treatment and seemed to be susceptible to stress factors in the BE, whereas taxa in the family *Acetobacteraceae* and other commensals such as *Bacillus* and *Staphylococcus* appear to be extraordinarily well-suited for survival under BE conditions.

BugBase [54] was used to validate the observed phenotypes for non-PMA and PMA samples (Fig. 3d). As compared with non-PMA samples, the PMA samples showed an increase in the relative abundance of aerobic (P_{adj} = 0.089) and facultative anaerobic communities (P_{adj} = 0.393), and a slight decrease in the abundance of anaerobic communities (P_{adj} = 0.217) (Fig. 3d). Interestingly, the abundance of taxa with stress-tolerant phenotypes increased in the PMA samples (P_{adj} = 0.063), indicating that microorganisms that could survive in the indoor environment might be better equipped to deal with BE-associated stress factors.

Archaea are an integral component of the BE

An archaea-centric approach [41] was taken to explore the archaeal communities present on the sampled surfaces. Overall, we obtained about 376,000 archaeal sequences in both PMA and non-PMA samples, which corresponded to 373 ASVs (on average 70.2 ± 22.8 ASVs/ house; 53.6 ± 16.8 ASVs/ non-PMA samples; 35.9 ± 22.1 ASVs/ PMA samples; Supplementary Tab. 9). The archaeal ASVs were classified into four different phyla, namely, Euryarchaeota (36.6% relative abundance in non-PMA samples, PMA: 35.0%), Thaumarchaeota (non-PMA: 62.2%, PMA: 64.1%), Crenarcheota (non-PMA: 0.8%, PMA: 0.5%) and Nanoarchaeota (non-PMA: 0.4%, PMA: 0.5%) (Fig. 4a).

On a family level, most reads were classified into the *Nitrososphaeraceae* (non-PMA: 62.1%, PMA: 64.1%), which is also the only archaeal family that was found in every household included in this study (Fig. 4c). In the *Nitrososphaeraceae*, the dominant genus identified was

Candidatus Nitrosocosmicus (non-PMA: 22.5%, PMA: 15.9%), but sequences classified within *Candidatus Nitrososphaera* (non-PMA: 0.9%, PMA: 0.2%) were also identified (Fig. 4b). The second-most abundant family was *Halococcaceae* (non-PMA: 19.7%, PMA: 28.7%), with *Halococcus* (non-PMA: 13.7%, PMA: 28.6%) identified as the predominant genus. One particularly fascinating finding was that oxygen-sensitive methanogenic taxa were detected in every household, but at a low relative abundance (*Methanobacteria** non-PMA: 3.7%, PMA: 3.5%; *Methanomicrobia** non-PMA: 4.0%, PMA: 2.6%), with *Methanosarcina** (non-PMA: 3.2%, PMA: 1.8%), *Methanobrevibacter** (non-PMA: 2.4%, PMA: 0.2%), *Methanobacterium** (non-PMA: 1.3%, PMA: 3.3%) and *Methanomassiliicoccus** (non-PMA: 0.4%, PMA: 0.2%) identified as the most abundant genera.

Humans are potentially the source of most archaeal taxa in the BE

The archaeal community composition suggests that some of the archaeal signatures identified on the bathroom surface could be of human origin, as *Thaumarchaeota*, *Haloarchaea* and methanogens have been previously associated with the human body [62]. Thus, we analysed the data obtained from these surfaces together with data obtained by applying the same archaea-centric approach to samples collected from the human body, namely, to stool (n = 38), urine (n = 43), nasal (n = 30), oral (n = 26), vaginal (n = 16) and skin (n = 7) samples (see Supplementary Tab. 5 and 9).

We recognised that indoor and human samples can be distinguished by their abundance and prevalence of *Thaumarchaeota* and *Euryarchaeota*, as *Thaumarchaeota* are highly enriched

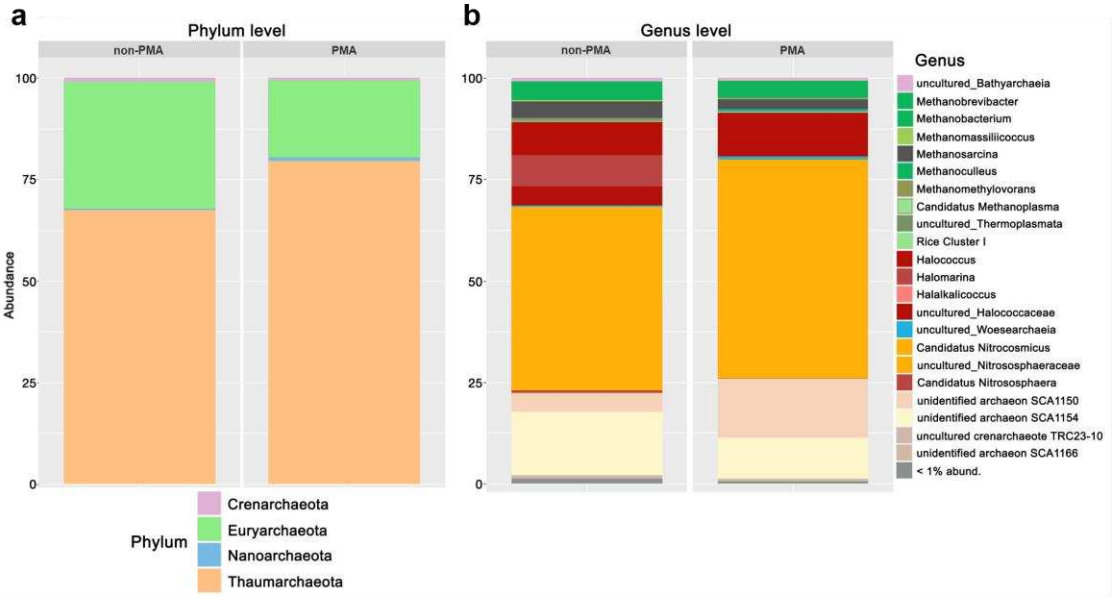

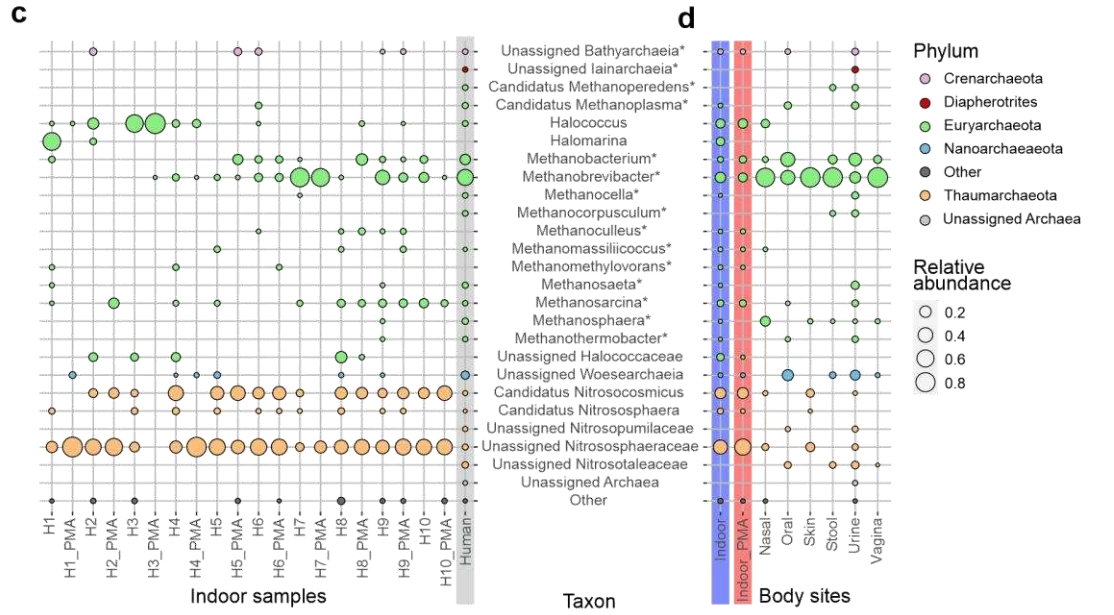

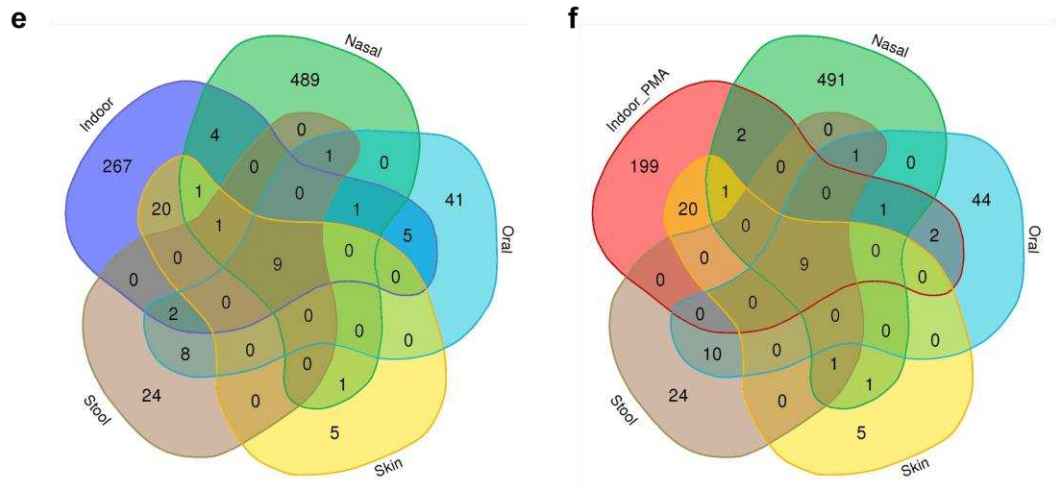

454

Fig. 4. Archaeal community composition in indoor samples. The relative abundance of archaeal taxa among 16S rRNA gene reads from bathroom floor surfaces at the **(a)** phylum and **(b)** genus levels. Bubble plot showing relative abundances of the 25 most-abundant archaeal genera found in bathroom and human samples: **(c)** Household samples (H1-H10) are depicted individually for non-PMA and PMA treatment of human samples (grey background) that represent reads from several body sites including nasal cavity, skin, vagina, urine, stool and oral samples. **(d)** Bubble plots of the 25 most-abundant archaeal genera, displayed according to their original samples. Relative abundance is reflected by the size of the bubbles. Genera are coloured according to their taxonomic phylum, and taxa that predominantly contain strict anaerobes are marked by an asterisk. Venn diagram of shared ASVs in **(e)** non-PMA indoor and **(f)** PMA indoor samples compared to nasal, oral, skin and stool samples (body sites that show the highest numbers of shared ASVs).

in indoor samples (P_{adj} = 3.5*10^{-11}; see Supplementary Fig. 5; Mann–Whitney *U* test), and *Euryarchaeota* are highly enriched in human samples (P_{adj} = 1.3*10^{-5}). This especially applies to signatures from *Candidatus Nitrososphaera* (P_{adj} = 2.9*10^{-26}) and *Cand. Nitrosocosmicus* (P_{adj} = 1.1*10^{-24}) that were rarely abundant in samples from the human body, but were often found in the analysed indoor samples. In addition, the relative abundance of unassigned *Nitrososphaeraceae* that were found in skin, urine and nasal samples was significantly higher (P_{adj} = 1.0*10^{-20}) in indoor samples.

Nevertheless, several archaeal genera were found in both indoor samples and human-associated samples. For example, reads classified as *Methanobacterium**, *Methanobrevibacter**, *Methanosarcina**, *Halococcus*, unassigned *Nitrososphaeraceae* and *Woesearchaeia* were present in both kinds of samples, indicating an overlap and that exchange is occurring between both microbiomes.

Venn diagrams were created to illustrate the number of shared archaeal ASVs between the indoor environments and all analysed body sites. Each sample type contained a certain number of specific ASVs (e.g. nasal samples: 489 ASVs, oral: 41 ASVs, skin: 5 ASVs, stool: 24 ASVs, indoor samples: 267 ASVs). The vaginal samples revealed only a small overlap with other samples with respect to the archaeal ASVs (15 unique ASVs, two shared with urine samples). Notably, nine ASVs (*Methanobrevibacter**) were shared across all sites, and the

483 skin samples shared the most (20) ASVs with the indoor environment (four *Candidatus*
484 *Nitrosocosmicus* ASVs and 16 ASVs uncultured *Nitrososphaeraceae*) (Fig. 4e,f).

485 In the next step, we examined the signatures of methanogenic archaea in more detail, as we
486 had used them as specific model microorganisms in our study. We were interested in
487 determining whether the methanogens identified in the indoor samples were of human origin
488 or were associated with archaeal signatures from the natural environment. Therefore, we first
489 extracted methanoarchaeal sequences from our indoor datasets (PMA and non-PMA) and
490 used these together with reference sequences from different environments that were available
491 from official databases to generate a phylogenetic tree (Fig. 5).

492 Most of the *Methanobrevibacter* sequences identified in the indoor samples clustered together
493 with host-associated (human (*M. smithii**, *M. oralis**), bovine/ovine (*M. millerae**), or biogas-
494 reactor/anaerobic-digestor-derived sequences, which are believed to be of holobiont origin.
495 Due to the fact that *Methanobrevibacter** is considered to be a strongly host-associated taxon
496 [32], we hypothesise that our detected *Methanobrevibacter** signatures are mostly derived
497 from human body-sites and only rarely from other, non-human environments.

498 Borrel et al. (2017) showed that nearly all human-associated *Methanomassiliicoccales** DNA
499 sequences clustered in a host-associated clade together with other *Methanomassiliicoccales**
500 sequences identified in animals, with the exception of two taxa, namely *Candidatus*
501 *Methanomassiliicoccus intestinalis** and *Methanomassiliicoccus luminyensis**. These two taxa
502 have been identified and isolated from human samples, but they cluster together with
503 sequences of microorganisms that are mainly associated with the soil and sediment
504 environment ("environmental clade"). This clearly shows that some environmental
505 *Methanomassiliicoccales** taxa can be transferred from the environment to the human body
506 and can colonise the human gut. The sequences assigned to the order of
507 *Methanomassiliicoccales** in our samples clustered only in the environment-associated clade
508 and were closer to the *Methanomassiliicoccales** sequences that have been identified in soils,
509 sediments and anaerobic digesters. Therefore, the external environment appears to be the

510 most probable source of the *Methanomassiliicoccales** sequences identified in our bathroom
511 floor samples.

512 Signatures of *Methanobacterium** are being more closely associated with human origin
513 [32,62]. Regarding *Methanobacterium**, we included sequences from environment- and
514 human-associated taxa in order to determine whether the *Methanobacterium** sequences
515 identified on the bathroom floor were of human origin or not. Most *Methanobacterium**
516 sequences identified in our human dataset clustered apart from all other *Methanobacterium**
517 sequences, with the exception of one ASV. This ASV clustered together with
518 *Methanobacterium ferruginis** and ASV49, which was identified in the non-PMA samples.
519 Seven ASVs from the PMA samples clustered with *Methanobacterium oryzae** and shared a
520 node with the phylogenetic group formed by the human-associated ASVs.

521 The results of phylogenetic and abundance-based analyses indicate that most of the identified
522 methanogenic sequences (and particularly *Methanobrevibacter** and *Methanobacterium**) in
523 the bathroom floor samples are probably indeed of human origin. This especially applies to
524 the identified sequences in indoor samples.

525

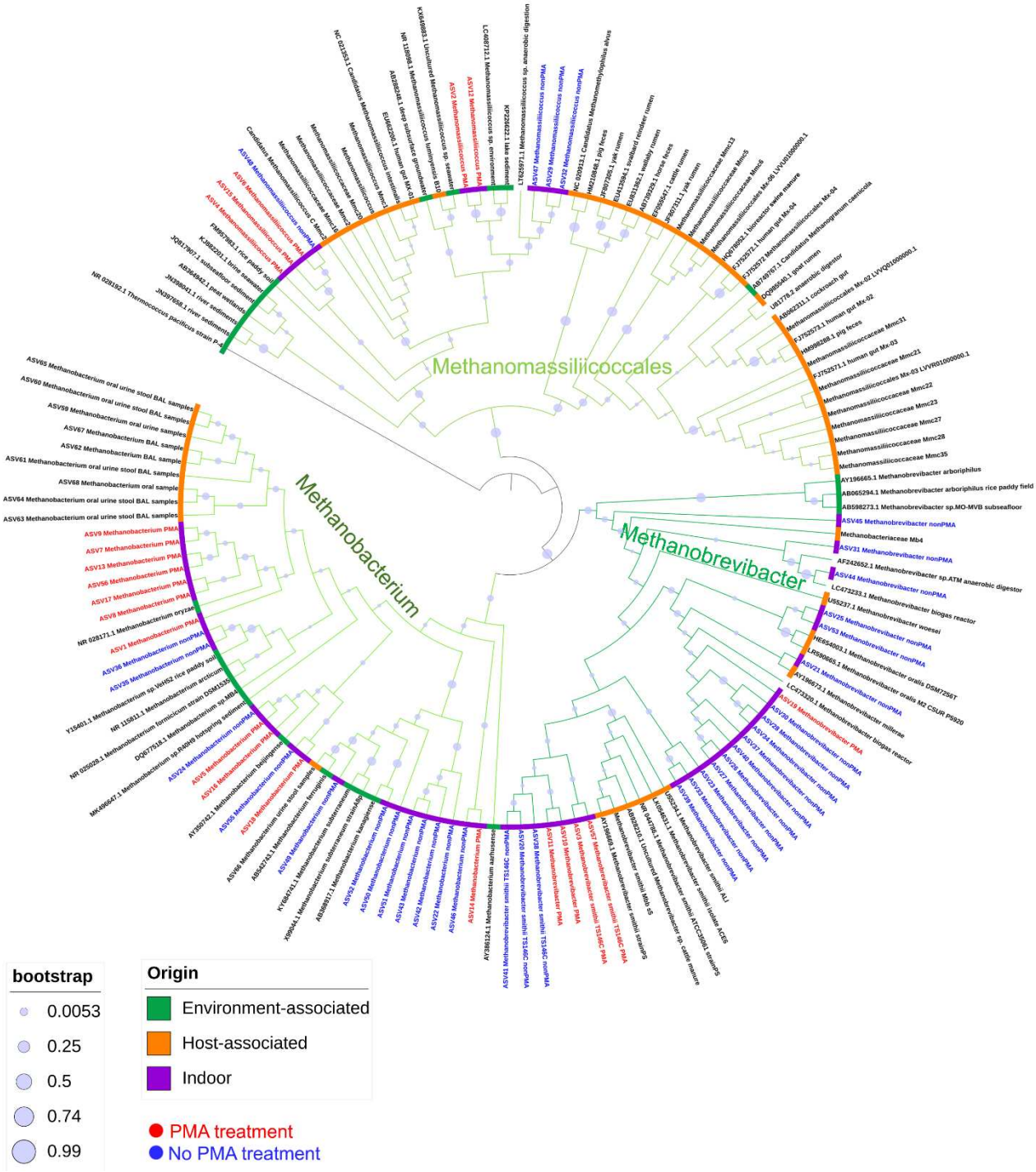

Fig. 5. Phylogenetic tree based on the sequences obtained from our study, NCBI and two other studies [5,56]**.** The circle indicates the origin of the sequences used to create the tree (see legend). The branches of the tree were coloured in different shades of green according to the taxa they represent.

Human-associated methanogens can survive oxygen exposure for up to 48 hours

Methanogenic archaea are strict anaerobes and are regarded as highly oxygen-sensitive. Nevertheless, in households with methanogenic taxa, we have frequently observed them in

both non-PMA and PMA samples, indicating that these taxa display a certain level of tolerance towards stress factors in the BE. Therefore, we performed an experimental analysis to determine whether methanogenic archaea, serving as models for strict anaerobic gastrointestinal microorganisms, were able to survive under aerial oxygen conditions and, therefore, potentially colonise the human body.

Three methanogen strains previously isolated from the human body, namely, *Methanobrevibacter smithii** (DSM no. 2375), *Methanosphaera stadtmanae** (DSM no. 3091), *Methanomassiliicoccus luminyensis** (DSM no. 25720) and one recently obtained isolate (*Methanobrevibacter sp.**; unpublished) from human faeces were exposed to aerobic and anoxic conditions over the period of up to 7 days (0 h, 6 h, 24 h, 48 h and 168 h). After exposure, the cells were transferred to fresh anoxic media and were allowed to grow for 2–3 weeks. Growth was then tested by measuring OD_{600} and methane production. All four strains could survive in the aerobic environment for at least 6 h (Fig. 6). *Methanomassiliicoccus luminyensis** was even able to survive for more than 48 h of exposure to aerobic conditions. No growth of *Methanomassiliicoccus luminyensis** was detected after 7 d of cultivation, under either anoxic or oxic conditions, indicating that other negative influences (e.g. starvation) potentially hindered the normal outgrowth.

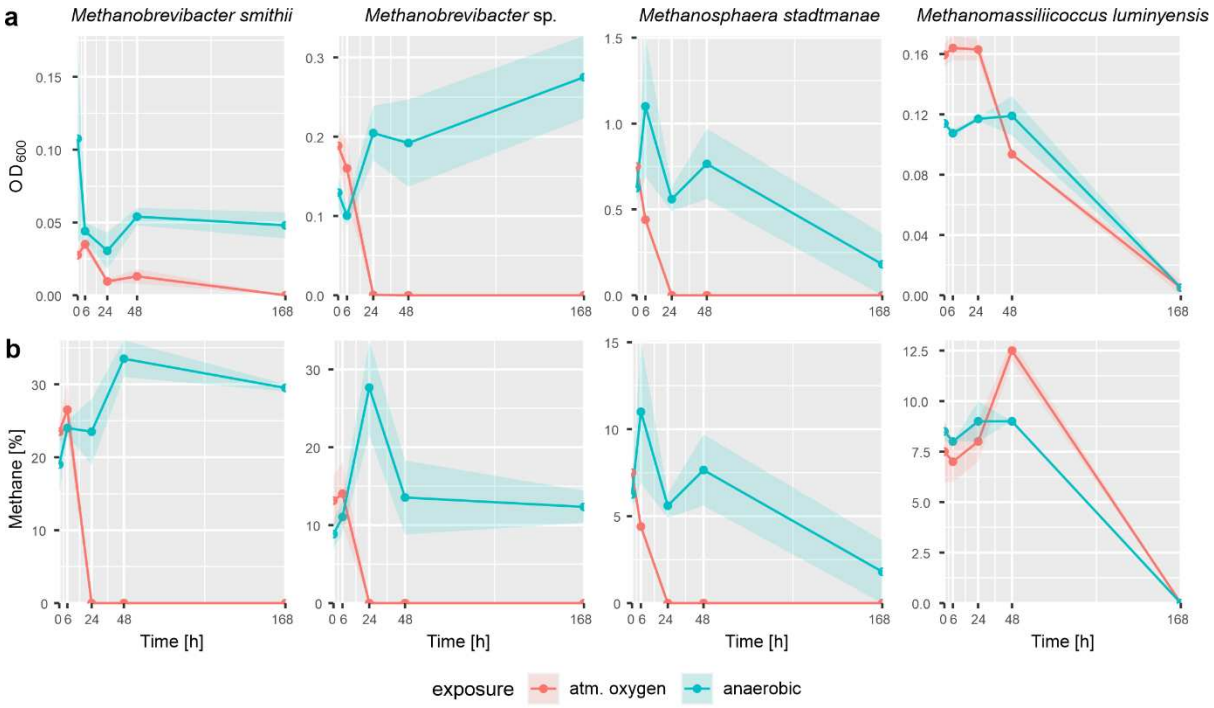

Fig. 6. Observed growth of selected human-associated methanogens after exposure to 21% oxygen (air). Plots indicate the growth as determined by **(a)** OD_{600} measurements and **(b)** methane production of the tested strains after exposure to an aerobic (red) or anaerobic (blue) environment for different periods of time ($n = 2$). The shaded areas represent the standard deviation.

To measure the genomic capacity of methanogens to resist oxygenic stress, we analysed the available representative genomes of *M. stadtmanae**, *M. smithii**, and *Methanomassiliicoccus** (Tab. 1). We specifically searched for keystone genes, as identified in Lyu and Lu (2018), and used the Microbial Genome Annotation and Analysis Platform (MaGe) for detailed comparative genomics [64].

Tab. 1. Genes for O_2/reactive oxygen species elimination enzymes and their presence in genomes of human-associated methanogens [63]**. Explanation of letters in brackets: (a)** protein inferred from homology, **(b)** predicted protein, **(c)** putative, **(d)** ferritin-like, **(e)** function from experimental evidence in other organisms, **(f)** ferritin, dps family protein. Specific gene identifiers derived from MaGe microscope database [64] and UniProtKB [65] are displayed in each column when present. n.d.: not detected.

	Methanosphaera stadtmanae		*Methanobrevibacter smithii*			*Methanomassiliicoccus*	
Enzyme	**DSM 3091**	**DEW79**	**DSM2374**	**DSM861**	**DSM 2375 (ALI)**	**M. luminyensis B10**	**M. intestinalis strain Issoire-Mx1**
Catalase (EC 1.11.1.6)	n.d.	n.d.	n.d.	n.d.	n.d.	CAJEv1_180010 (e)	MMINT_12710 (a) MMINT_12690 (a)
Peroxiredoxin (EC 1.11.1.24)	n.d.	n.d.	n.d.	n.d.	n.d.	CAJEv1_50026	MMINT_19160 (a) MMINT_05530 (b) MMINT_15900 (b)
Rubrerythrin	Msp_0789 (b)	n.d.	METSMIF1_02444 (b)	Msm_1733 (b) Msm_1348 (b)	METSMIALI_01290 (b)	CAJEv1_240034 (e)	MMINT_05220 (b) MMINT_00570 (b)
Superoxide dismutase (EC 1.15.1.1)	n.d.	n.d.	n.d.	n.d.	n.d.	CAJEv1_120763 (e)	n.d.
Superoxide reductase	n.d.	n.d.	METSMIF1_03626 (a,c)	n.d.	METSMIALI_00110 (a,c)	n.d.	n.d.
$F_{420}H_2$ oxidase	n.d.	n.d.	n.d.	Msm_1349 (b)	n.d.	n.d.	n.d.
NO/O_2 reductase	n.d.	n.d.	n.d.	n.d.	n.d.	CAJEv1_120660 (e)	n.d.
Ferritin	Msp_0852 (a, b)	n.d.	METSMIF1_03296 (a,d)	Msm_1712 (a, b)	METSMIALI_00411 (a,d)	CAJEv1_120620 (e, f)	MMINT_08340 (a, f)
Thioredoxin	Msp_0103 (a,c) Msp_0820 (a,c)	n.d.	METSMIF1_02203 (a)	Msm_0838 (a, c)	METSMIALI_01538 (a)	CAJEv1_200051 CAJEv1_230019 (c,) CAJEv1_240002	MMINT_17530 (b) MMINT_19530 (b)
Rubredoxin (EC 1.4.3)	Msp_0445 (a) Msp_0444 (a)	n.d.	METSMIF1_03551 (a) METSMIF1_03550 (b) METSMIF1_03395 (a) METSMIF1_03318 (b)	Msm_0187 (b) Msm_0188 (a)	METSMIALI_00388 (b) METSMIALI_00192 (b) METSMIALI_00191 (a) METSMIALI_00344 (a)	CAJEv1_120430 (e)	MMINT_08590 (a)
UniProtKB	UniProtKB	UniProtKB	UniProtKB	UniProtKB	UniProtKB	MAGE	UniProtKB

All investigated methanogens (except DEW79) revealed the presence of rubrerythrin, ferritin, thioredoxin and rubredoxin in their genomic inventory. The extended survival under oxygenated conditions for *Methanomassiliicoccus** was supported by the detection of catalase and peroxiredoxin, as well as superoxide dismutase in the case of *M. luminyensis**.

Overall, the experimental and database-derived results show that human-associated archaea have profound capacities to survive under oxygenated conditions for a minimum of 6 hours.

Discussion

The viability of microorganisms that exist in indoor environments is of great interest [11], as a substantial number of microorganisms are in constant exchange with the human body [15,66–68]. These interactions between humans and (viable) microbes are arguably of crucial importance for training the immune system and sensitisation in infants [69], as well as the recolonisation of the human microbiome after antibiotic intervention or disease [17,18].

Our study findings support the hypothesis that the indoor surfaces of normal houses harbour unique microbial communities [66]. The single household profiles are largely dominated by human microbial signatures while environmental taxa play minor roles (for comparison, please see Adams et al., 2015; Chase et al., 2016; Hewitt et al., 2012; Jeon et al., 2013; Rintala et al., 2008), (Fig. 3). This finding is in agreement with the concept of a personalised microbial cloud that mediates the transfer to surfaces [74]. In particular, we identified the skin microbiome as a major contributor to this cloud (~40%), even in areas close to the toilet, as has been shown in previous studies [37,38,73,75]. Although we observed substantial variation among the microbial communities in the ten households, approximately 30% of the overall microbial community detected on bathroom floors consisted of microbiomes from faecal, vaginal and urinary origins. The presence of those microbial taxa can be explained by the production of aerosols by toilet flushing [76]. However, closing the toilet lid prior to flushing, as is practised in households H4 and H10, did not substantially alter the proportions of contributing body sites. This result raises the question of whether other possible sources of those microbes exist, such as the shower [77] or the sink [36].

Molecular surveys of the BE microbiome usually do not discriminate between viable and dead microbes. As DNA is highly stable in the environment, and microbial signatures remain detectable for a long time, the presence of DNA signatures alone does not serve as a good indicator for viability and metabolic activity per se. Once dispersed, DNA traces of human gut- and skin-associated taxa can still be tracked on public restroom floors and walls after a period of several weeks [37]. Thus, the proportion of relevant microorganisms in the BE might be overestimated when conventional microbiome approaches are taken. Cultivation-based assays, however, are hindered by their technological limitations and might only reflect a non-representative proportion of living indoor microbiota [11].

In this study, we analysed specifically the intact floor microbial community and determined the quality and quantity of the potential microbial ex-host survivors by using PMA treatment, which has rarely been applied to BE environment samples so far [78–80]. One previous specific

application was the assessment of living microorganisms in the vicinity of spacecraft, a study that was carried out to understand the risk of contamination for extra-terrestrial research targets (planetary protection; Mahnert et al., 2015; Moissl-Eichinger et al., 2015). Notably, a proportion of 1–45% of the detected microbial community was deemed to be potentially alive under (stringent) cleanroom conditions [79,81].

Our experiment revealed that the majority of detected microbial signatures originated from disintegrated cells or free DNA. More specifically, we observed a more than 3- and 4-fold decrease in the absolute number of 16S rRNA genes analysed via qPCR for archaea and bacteria, respectively, upon the PMA-treatment of bathroom floor samples (Fig. 3). However, these results also imply that less than 25% of the microbial signatures originate from intact, and likely living, cells that are potentially able to colonise the human body after seven days of regular contact to a human host. The potentially living cells detected in PMA samples could be associated with a predominantly aerobic lifestyle and increased stress tolerance, and these cells could include aerobic, human- and environment-associated, but also spore-forming taxa. The predominance of aerotolerant and spore-forming taxa in PMA samples supports the hypothesis that microbes do not proliferate, but instead persist in the BE as a result of accumulation and dormancy [82].

Whether obligatory anaerobic human commensals can be transmitted between individuals via the BE is still an open question. Notably, microbial taxa such as clostridia might not be directly transmitted from mother to child, even though strains of clostridia are the most abundant bacterial group in the maternal gut [83]. Korpela and de Vos (2018) argued that clostridia may rely on transmission via relatives or non-direct transmission between hosts (i.e. transmission via the environment). This argument is supported by our observation that spore formers, including clostridia, have a perceived increase in survival rate, and seem to be able to survive oxygen exposure and potentially the acidic environment of the stomach.

632 This kind of horizontal, indirect transfer may be a very rare event in healthy adults, as the
633 transmission success depends on several factors, such as transmission routes, dispersal
634 efficiency, the ability to survive “ex-host”, human colonisation resistance, and the ability of gut
635 commensals to survive gastric and bile acids [1]. These factors are largely unexplored for
636 commensals, but it can be assumed that pathogens and commensals use similar
637 mechanisms. For example, the transmission routes of many pathogens are well-known and
638 primarily include the direct inhalation of aerosols and dust (e.g. *Bacillus anthracis*,
639 *Mycobacterium tuberculosis*) or surface contact (e.g. *Clostridium difficile**, *Staphylococcus*
640 *aureus*, *Enterococcus faecalis*) [11]. It is likely that human commensals also use such
641 mechanisms for transmission. However, such a transmission could not be verified within the
642 scope of our study and has to be evaluated in further surveys by performing a microbial
643 genomic sequence variation analysis to gather evidence for the transfer of commensals
644 between individuals and the BE.

645 One intriguing results of this study was the detection of archaea as integral components of the
646 BE microbiome. Even though archaea were outnumbered by bacteria nearly 100-fold, they
647 were found in every PMA-treated household sample. Especially taxa of the family
648 *Nitrososphaeraceae* were highly predominant in PMA and non-PMA samples and seem to be
649 relatively stable components of the BE. In contrast, *Euryarchaeota* appeared to be only
650 transient occupants of the indoor microbiome, as many genera were limited to a few
651 households, and their signals frequently disappeared in PMA samples.

652 An exception to this pattern was observed for the taxon *Methanobrevibacter**, which is the
653 most abundant human archaeal genus in the GIT [62]. *Methanobrevibacter** signatures were
654 found on all analysed human body sites and in seven out of ten household samples in both
655 PMA and non-PMA samples. These results appear to contradict the general assumption that
656 methanogens are highly oxygen-sensitive [84–87]. However, although taxa of the
657 *Methanobacteriales** family seem to be susceptible to ROS [63], analyses of experimental
658 data reveal that methanogens can survive oxygen exposure for periods of several hours to

659 days [88,89] and are capable to recover from reoccurring aerobic conditions in the
660 environment such as alternated wet and dry rice paddy fields [90–92].

661 By performing experiments with representative human GIT methanogens, we could confirm
662 that *M. smithii* species* and *M. stadtmanae** survived aeration conditions for more than 6
663 hours, while *M. luminyensis** even endured oxygen exposure for more than 48 hours under
664 our experimental conditions (see Fig. 6). The ability of methanogens to endure aerobic
665 conditions was supported by a genomic analysis of common pathways to detoxify ROS. All
666 analysed human-associated methanogens, except *Methanosphaera stadtmanae* strain
667 DEW79, possessed key genes for enzymes such as rubrerythrin, ferritin, thioredoxin and
668 rubredoxin, all of which enable organisms to survive in aerobic environments (see Tab. 1).
669 *Methanomassiliicoccus* sp. further exhibits genes that encode for putative peroxidases and
670 catalases, indicating that this taxon has the potential to deal with ROS, as indicated by our
671 experimental approach.

672 We are aware, that our study results need to be regarded under the aspect of some
673 methodological limitations. PMA is a powerful tool to mask free DNA but can be affected in its
674 efficacy via physiochemical properties of the sample (e.g. pH, turbidity, optical density) and
675 biochemical characteristics of the microbial community itself (e.g. cell wall structures, natural
676 intake and efflux mechanisms) [40,80]. In context of this study, we analysed relatively clean,
677 matrix-free BE samples with rather low biomass, suggesting that our results potentially
678 underestimate the amount and diversity of intact microbes in the BE according to a recent
679 evaluation of Wang et al. (2021) [93]. We are thus very confident that the taxa we identified in
680 the PMA dataset originate from intact cells, even though it is still conceivable that some of the
681 taxa found in the PMA dataset are “PMA-resilient”. In our dataset, this may particularly apply
682 for the genera *Corynebacterium* and *Staphylococcus* that have been shown to be fairly
683 unresponsive to PMA treatment [93]. Further limitations include our small sample size and the
684 high level of heterogeneity among the different households which serves as a source of
685 potential bias. In this study, we did not analyse other surfaces/house areas (such as showers

686 or sinks, door handles, dust etc.), which would be of interest in future studies to obtain a better
687 overall picture [36,73]. Due to the limitations of amplicon sequencing, it was not possible to
688 retrieve functional data for the analyses, i.e. to speculate on the abilities of the microbiome to
689 deal with environmental stress factors. Other techniques, such as shotgun metagenomics,
690 that allow for taxonomic and functional analyses could be employed in future PMA-based BE
691 surveys to obtain such functional data. In addition, environmental, physical parameters such
692 as humidity, temperature, or the frequency of ventilation in the BE should be tracked, as these
693 could help explain microbial survival [94,95].

694 By taking into account both 16S rRNA gene amplicon sequencing and experimental
695 approaches, we gathered evidence that supports the hypothesis that methanogens can
696 endure aerobic conditions for a limited amount of time. This introduces a new potential
697 transmission pathway, which is especially interesting with respect to infants, as it presents
698 another way in which they can acquire microbes aside from direct seeding during vaginal birth.
699 It is still not know whether methanogens such as *Methanobrevibacter** are acquired perinatal
700 and escape detection early in life or colonise the GIT via another source, such as the BE or
701 dietary products like yoghurt, organic milk and vegetables [96–99]. The latter scenario is
702 plausible, as methanogens co-evolved with animals [56,100] and, thus, have adapted to the
703 human GIT.

704 Conclusions

705 In conclusion, this study enabled us to use PMA treatment together with molecular quantitative
706 and qualitative methods to successfully assess the survival of Bacteria and Archaea on indoor
707 surfaces. The results indicate that one-fifth of the bathroom surface microbiome is intact or
708 even alive. As even strict anaerobes, such as oxygen-sensitive methanogenic archaea, were
709 found to be intact and potentially alive despite their exposure to the fully aerated environment,
710 we conclude that these microorganisms may represent a valid source for human microbiome

711 constituents, even though a direct colonisation from BE to human needs to be verified in a
712 subsequent study.

713

714 Availability of data and materials

715 The datasets supporting the conclusions of this article are available in the European
716 Nucleotide Archive (ENA) repository, Primary Accession: PRJEB41618 in
717 https://www.ebi.ac.uk/. Further details can be found in Supplementary Table 4. The R script
718 for the generation of bubble plots was used and adapted from https://github.com/alex-
719 bagnoud/OTU-table-to-bubble-plot.

720

721 Abbreviations

722	ASV:	amplicon sequence variant
723	BE:	built environment
724	Cp:	crossing point
725	GIT:	gastrointestinal tract
726	LEfSe:	Linear discriminant analysis Effect Size
727	MaGe:	Microbial Genome Annotation and Analysis Platform
728	OD:	optical density
729	PCoA:	principal coordinates analysis
730	PMA:	propidium monoazide
731	qPCR:	quantitative polymerase chain reaction
732	ROS:	reactive oxygen species
733	TSS:	total sum normalisation

Acknowledgements

We thank the participants of our study by providing samples from their bathroom floors. We thank Charlotte Neumann and Christina Kumpitsch for critical proof-reading. Manuela Pausan and Marcus Blohs are students of the local PhD doctoral program “MolMed”. The authors acknowledge the support of the ZMF Galaxy Team: Core Facility Computational Bioanalytics, Medical University of Graz, funded by the Austrian Federal Ministry of Education, Science and Research, Hochschulraum-Strukturmittel 2016 grant as part of BioTechMed Graz.

Funding

The project was supported financially by the local PhD doctoral program “MolMed”.

Author information

Affiliations

Diagnostic and Research Institute of Hygiene, Microbiology and Environmental Medicine, Medical University of Graz, Graz 8010, Austria

M. Blohs, A. Mahnert, C. Moissl-Eichinger

Steigerwald Arzneimittelwerk GmbH, Bayer Consumer Health, Havelstrasse 5, D-64295 Darmstadt, Germany

M.-R. Pausan

752 **Authors´ contributions**

753 MRP and MB contributed equally to this work. MRP, CME: study design and phylogenetic
754 analysis. MRP: sampling, biological samples processing, collection of metadata, microbiome
755 data analysis, contributed to manuscript writing. MB: analysis of microbiome data and
756 statistical analysis, wrote manuscript. AM: support of microbiome data and statistical analysis.
757 CME: genome mining, wrote manuscript.

758 **Corresponding author**

759 Correspondence to C. Moissl-Eichinger.

760 Ethics declarations

761 **Ethics approval and consent to participate**

762 Ethical approval for the study was obtained from the ethics committee of the Medical University
763 Graz. Written informed consent was obtained from all participants. Ethic approvals for the
764 respective body sites are listed in the Supplementary Table 4.

765 **Consent for publication**

766 Not applicable.

767 **Competing interests**

768 The authors declare that they have no competing interests.

769

770

References

1. Browne HP, Neville BA, Forster SC, Lawley TD. Transmission of the gut microbiota: Spreading of health. Nat Rev Microbiol [Internet]. Nature Publishing Group; 2017;15:531–43. Available from: http://dx.doi.org/10.1038/nrmicro.2017.50

2. Stewart CJ, Ajami NJ, O'Brien JL, Hutchinson DS, Smith DP, Wong MC, et al. Temporal development of the gut microbiome in early childhood from the TEDDY study. Nature [Internet]. Springer US; 2018;562:583–8. Available from: http://dx.doi.org/10.1038/s41586-018-0617-x

3. Guaraldi F, Salvatori G. Effect of Breast and Formula Feeding on Gut Microbiota Shaping in Newborns. Front Cell Infect Microbiol [Internet]. Adlerberth; 2012 [cited 2020 Nov 25];2:94. Available from: http://journal.frontiersin.org/article/10.3389/fcimb.2012.00094/abstract

4. Moossavi S, Azad MB. Origins of human milk microbiota: new evidence and arising questions. Gut Microbes [Internet]. NLM (Medline); 2020 [cited 2020 Nov 25];12:1667722. Available from: https://www.tandfonline.com/doi/full/10.1080/19490976.2019.1667722

5. Pasolli E, Asnicar F, Manara S, Zolfo M, Karcher N, Armanini F, et al. Extensive Unexplored Human Microbiome Diversity Revealed by Over 150,000 Genomes from Metagenomes Spanning Age, Geography, and Lifestyle. Cell [Internet]. Cell Press; 2019 [cited 2020 Nov 25];176:649-662.e20. Available from: https://pubmed.ncbi.nlm.nih.gov/30661755/

6. Rocchi S, Reboux G, Scherer E, Laboissière A, Zaros C, Rouzet A, et al. Indoor microbiome: Quantification of exposure and association with geographical location, meteorological factors, and land use in France. Microorganisms. MDPI AG; 2020;8.

7. Koenig JE, Spor A, Scalfone N, Fricker AD, Stombaugh J, Knight R, et al. Succession of microbial consortia in the developing infant gut microbiome. Proc Natl Acad Sci U S A [Internet]. National Academy of Sciences; 2011 [cited 2021 Mar 17];108:4578–85. Available from: www.pnas.org/cgi/doi/10.1073/pnas.1000081107

8. Yatsunenko T, Rey FE, Manary MJ, Trehan I, Dominguez-Bello MG, Contreras M, et al. Human gut microbiome viewed across age and geography [Internet]. Nature. Nature Publishing Group; 2012 [cited 2021 Mar 17]. p. 222–7. Available from: https://www.nature.com/articles/nature11053

9. Chase J, Fouquier J, Zare M, Sonderegger DL, Knight R, Kelley ST, et al. Geography and Location Are the Primary Drivers of Office Microbiome Composition. mSystems [Internet]. American Society for Microbiology; 2016 [cited 2020 Nov 25];1:1–18. Available from: http://msystems.asm.org/

10. Dannemiller KC. Moving towards a Robust Definition for a "Healthy" Indoor Microbiome. mSystems. 2019;4:1–5.

11. Gilbert JA, Stephens B. Microbiology of the built environment. Nat Rev Microbiol [Internet]. Springer US; 2018 [cited 2020 Dec 1];16:661–70. Available from: http://dx.doi.org/10.1038/s41579-018-0065-5

12. Horve PF, Lloyd S, Mhuireach GA, Dietz L, Fretz M, MacCrone G, et al. Building upon current knowledge and techniques of indoor microbiology to construct the next era of theory into microorganisms, health, and the built environment. J Expo Sci Environ Epidemiol

812 [Internet]. Springer US; 2020;30:219–35. Available from: http://dx.doi.org/10.1038/s41370-
813 019-0157-y

814 13. Kelley ST, Gilbert JA. Studying the microbiology of the indoor environment [Internet].
815 Genome Biol. BioMed Central Ltd.; 2013 [cited 2020 Dec 1]. Available from:
816 https://pubmed.ncbi.nlm.nih.gov/23514020/

817 14. Klepeis NE, Nelson WC, Ott WR, Robinson JP, Tsang AM, Switzer P, et al. The National
818 Human Activity Pattern Survey (NHAPS): A resource for assessing exposure to environmental
819 pollutants. J Expo Anal Environ Epidemiol. 2001;11:231–52.

820 15. Brooks B, Firek BA, Miller CS, Sharon I, Thomas BC, Baker R, et al. Microbes in the
821 neonatal intensive care unit resemble those found in the gut of premature infants. Microbiome
822 [Internet]. 2014;2:1. Available from: http://www.microbiomejournal.com/content/2/1/1

823 16. Brooks AW, Priya S, Blekhman R, Bordenstein SR. Gut microbiota diversity across
824 ethnicities in the United States. Cadwell K, editor. PLOS Biol [Internet]. Public Library of
825 Science; 2018 [cited 2020 Nov 25];16:e2006842. Available from:
826 https://dx.plos.org/10.1371/journal.pbio.2006842

827 17. Ng KM, Aranda-Díaz A, Tropini C, Frankel MR, Van Treuren W, O'Laughlin CT, et al.
828 Recovery of the Gut Microbiota after Antibiotics Depends on Host Diet, Community Context,
829 and Environmental Reservoirs. Cell Host Microbe. Cell Press; 2019;26:650-665.e4.

830 18. Parajuli A, Hui N, Puhakka R, Oikarinen S, Grönroos M, Selonen VAO, et al. Yard
831 vegetation is associated with gut microbiota composition. Sci Total Environ. Elsevier B.V.;
832 2020;713:136707.

833 19. Mahnert A, Moissl-Eichinger C, Zojer M, Bogumil D, Mizrahi I, Rattei T, et al. Man-made
834 microbial resistances in built environments. Nat Commun [Internet]. Springer US; 2019;10:1–
835 12. Available from: http://dx.doi.org/10.1038/s41467-019-08864-0

836 20. Mora M, Mahnert A, Koskinen K, Pausan MR, Oberauner-Wappis L, Krause R, et al.
837 Microorganisms in confined habitats: Microbial monitoring and control of intensive care units,
838 operating rooms, cleanrooms and the international space station. Front Microbiol. 2016;7:1–
839 20.

840 21. Lax S, Sangwan N, Smith D, Larsen P, Handley KM, Richardson M, et al. Bacterial
841 colonization and succession in a newly opened hospital. Sci Transl Med. 2017;9:1–12.

842 22. Ege MJ, Mayer M, Schwaiger K, Mattes J, Pershagen G, Van Hage M, et al. Environmental
843 bacteria and childhood asthma. Allergy Eur J Allergy Clin Immunol. 2012;67:1565–71.

844 23. Dannemiller KC, Mendell MJ, Macher JM, Kumagai K, Bradman A, Holland N, et al. Next-
845 generation DNA sequencing reveals that low fungal diversity in house dust is associated with
846 childhood asthma development. Indoor Air. 2014;24:236–47.

847 24. Kirjavainen P V., Karvonen AM, Adams RI, Täubel M, Roponen M, Tuoresmäki P, et al.
848 Farm-like indoor microbiota in non-farm homes protects children from asthma development.
849 Nat Med. 2019;25:1089–95.

850 25. Costello EK, Stagaman K, Dethlefsen L, Bohannan BJM, Relman DA. The application of
851 ecological theory toward an understanding of the human microbiome. Science (80-).
852 2012;336:1255–62.

853 26. Eckburg PB, Bik EM, Bernstein CN, Purdom E, Dethlefsen L, Sargent M, et al.
854 Microbiology: Diversity of the human intestinal microbial flora. Science (80-) [Internet]. NIH
855 Public Access; 2005 [cited 2020 Nov 25];308:1635–8. Available from:
856 /pmc/articles/PMC1395357/?report=abstract

857 27. Ley RE, Lozupone CA, Hamady M, Knight R, Gordon JI. Worlds within worlds: Evolution
858 of the vertebrate gut microbiota. Nat Rev Microbiol [Internet]. Nat Rev Microbiol; 2008 [cited
859 2020 Nov 25];6:776–88. Available from: https://pubmed.ncbi.nlm.nih.gov/18794915/

860 28. Meehan CJ, Beiko RG. A phylogenomic view of ecological specialization in the
861 lachnospiraceae, a family of digestive tract-associated bacteria. Genome Biol Evol [Internet].
862 Oxford University Press; 2014 [cited 2020 Nov 25];6:703–13. Available from:
863 https://pubmed.ncbi.nlm.nih.gov/24625961/

864 29. Browne HP, Forster SC, Anonye BO, Kumar N, Neville BA, Stares MD, et al. Culturing of
865 “unculturable” human microbiota reveals novel taxa and extensive sporulation. Nature
866 [Internet]. Nature Publishing Group; 2016 [cited 2021 Mar 17];533:543–6. Available from:
867 https://www.nature.com/articles/nature17645

868 30. Rolfe RD, Hentges DJ, Campbell BJ, Barrett JT. Factors related to the oxygen tolerance
869 of anaerobic bacteria. Appl Environ Microbiol. 1978;36:306–13.

870 31. Miller RA, Britigan BE. Role of oxidants in microbial pathophysiology [Internet]. Clin.
871 Microbiol. Rev. American Society for Microbiology; 1997 [cited 2020 Nov 25]. p. 1–18.
872 Available from: /pmc/articles/PMC172912/?report=abstract

873 32. Maria Chibani C, Mahnert A, Borrel G, Almeida A, Werner A, Brugère J-F, et al. A
874 comprehensive analysis of the global human gut archaeome from a thousand genome
875 catalogue. bioRxiv [Internet]. Cold Spring Harbor Laboratory; 2020 [cited 2020 Nov
876 25];2020.11.21.392621. Available from: https://doi.org/10.1101/2020.11.21.392621

877 33. Dridi B, Henry M, El Khéchine A, Raoult D, Drancourt M. High prevalence of
878 Methanobrevibacter smithii and Methanosphaera stadtmanae detected in the human gut using
879 an improved DNA detection protocol. PLoS One. 2009;4.

880 34. Palmer C, Bik EM, DiGiulio DB, Relman DA, Brown PO. Development of the human infant
881 intestinal microbiota. PLoS Biol. 2007;5:1556–73.

882 35. Wampach L, Heintz-Buschart A, Hogan A, Muller EEL, Narayanasamy S, Laczny CC, et
883 al. Colonization and succession within the human gut microbiome by archaea, bacteria, and
884 microeukaryotes during the first year of life. Front Microbiol. 2017;8:1–21.

885 36. Dunn RR, Fierer N, Henley JB, Leff JW, Menninger HL. Home Life: Factors Structuring
886 the Bacterial Diversity Found within and between Homes. PLoS One. 2013;8.

887 37. Gibbons SM, Schwartz T, Fouquier J, Mitchell M, Sangwan N, Gilbert JA, et al. Ecological
888 succession and viability of human-associated microbiota on restroom surfaces. Appl Environ
889 Microbiol. 2015;81:765–73.

890 38. Flores GE, Bates ST, Knights D, Lauber CL, Stombaugh J, Knight R, et al. Microbial
891 biogeography of public restroom surfaces. PLoS One. 2011;6.

892 39. Mora M, Perras A, Alekhova TA, Wink L, Krause R, Aleksandrova A, et al. Resilient
893 microorganisms in dust samples of the International Space Station-survival of the adaptation
894 specialists. Microbiome [Internet]. BioMed Central; 2016 [cited 2021 Mar 14];4:65. Available

from: https://link.springer.com/articles/10.1186/s40168-016-0217-7

40. Nocker A, Sossa-Fernandez P, Burr MD, Camper AK. Use of propidium monoazide for live/dead distinction in microbial ecology. Appl Environ Microbiol [Internet]. American Society for Microbiology (ASM); 2007 [cited 2020 Nov 25];73:5111–7. Available from: /pmc/articles/PMC1951001/?report=abstract

41. Pausan MR, Csorba C, Singer G, Till H, Schöpf V, Santigli E, et al. Exploring the Archaeome: Detection of Archaeal Signatures in the Human Body. Front Microbiol [Internet]. Frontiers Media S.A.; 2019 [cited 2020 Nov 25];10:2796. Available from: https://www.frontiersin.org/article/10.3389/fmicb.2019.02796/full

42. Probst AJ, Auerbach AK, Moissl-Eichinger C. Archaea on Human Skin. PLoS One. 2013;8.

43. Bolyen E, Rideout JR, Dillon MR, Bokulich NA, Abnet CC, Al-Ghalith GA, et al. Reproducible, interactive, scalable and extensible microbiome data science using QIIME 2 [Internet]. Nat. Biotechnol. Nature Publishing Group; 2019 [cited 2020 Nov 25]. p. 852–7. Available from: https://pubmed.ncbi.nlm.nih.gov/31341288/

44. Mahnert A, Verseux C, Schwendner P, Koskinen K, Kumpitsch C, Blohs M, et al. Microbiome dynamics during the HI-SEAS IV mission, and implications for future crewed missions beyond Earth. 2020;

45. Callahan BJ, McMurdie PJ, Rosen MJ, Han AW, Johnson AJA, Holmes SP. DADA2: High-resolution sample inference from Illumina amplicon data. Nat Methods [Internet]. Nature Publishing Group; 2016 [cited 2020 Nov 25];13:581–3. Available from: https://pubmed.ncbi.nlm.nih.gov/27214047/

46. Bokulich NA, Kaehler BD, Rideout JR, Dillon M, Bolyen E, Knight R, et al. Optimizing taxonomic classification of marker-gene amplicon sequences with QIIME 2's q2-feature-classifier plugin. Microbiome [Internet]. BioMed Central Ltd.; 2018 [cited 2020 Dec 1];6:90. Available from: https://microbiomejournal.biomedcentral.com/articles/10.1186/s40168-018-0470-z

47. Quast C, Pruesse E, Yilmaz P, Gerken J, Schweer T, Yarza P, et al. The SILVA ribosomal RNA gene database project: Improved data processing and web-based tools. Nucleic Acids Res [Internet]. Oxford University Press; 2013 [cited 2020 Nov 25];41:D590. Available from: /pmc/articles/PMC3531112/?report=abstract

48. Caporaso JG, Lauber CL, Walters WA, Berg-Lyons D, Lozupone CA, Turnbaugh PJ, et al. Global patterns of 16S rRNA diversity at a depth of millions of sequences per sample. Proc Natl Acad Sci U S A [Internet]. National Academy of Sciences; 2011 [cited 2020 Nov 25];108:4516–22. Available from: www.pnas.org/cgi/doi/10.1073/pnas.1000080107

49. Walters W, Hyde ER, Berg-Lyons D, Ackermann G, Humphrey G, Parada A, et al. Improved Bacterial 16S rRNA Gene (V4 and V4-5) and Fungal Internal Transcribed Spacer Marker Gene Primers for Microbial Community Surveys. mSystems [Internet]. American Society for Microbiology; 2016 [cited 2020 Nov 25];1. Available from: http://msystems.asm.org/

50. McMurdie PJ, Holmes S. phyloseq: An R Package for Reproducible Interactive Analysis and Graphics of Microbiome Census Data. Watson M, editor. PLoS One [Internet]. Public Library of Science; 2013 [cited 2020 Nov 26];8:e61217. Available from: https://dx.plos.org/10.1371/journal.pone.0061217

938 51. Wickham H. ggplot2: Elegant Graphics for Data Analysis [Internet]. Springer-Verlag New
939 York; 2016. Available from: https://ggplot2.tidyverse.org

940 52. Benjamini Y, Hochberg Y. Controlling the False Discovery Rate: A Practical and Powerful
941 Approach to Multiple Testing. Source J. R. Stat. Soc. Ser. B. 1995.

942 53. Zakrzewski M, Proietti C, Ellis JJ, Hasan S, Brion MJ, Berger B, et al. Calypso: A user-
943 friendly web-server for mining and visualizing microbiome-environment interactions.
944 Bioinformatics [Internet]. Oxford University Press; 2017 [cited 2020 Nov 29];33:782–3.
945 Available from: /pmc/articles/PMC5408814/?report=abstract

946 54. Ward T, Larson J, Meulemans J, Hillmann B, Lynch J, Sidiropoulos D, et al. BugBase
947 predicts organism-level microbiome phenotypes [Internet]. bioRxiv. bioRxiv; 2017 [cited 2020
948 Nov 25]. p. 133462. Available from: https://doi.org/10.1101/133462

949 55. Knights D, Kuczynski J, Charlson ES, Zaneveld J, Mozer MC, Collman RG, et al. Bayesian
950 community-wide culture-independent microbial source tracking. Nat Methods [Internet]. NIH
951 Public Access; 2011 [cited 2020 Nov 25];8:761–5. Available from:
952 /pmc/articles/PMC3791591/?report=abstract

953 56. Borrel G, McCann A, Deane J, Neto MC, Lynch DB, Brugère JF, et al. Genomics and
954 metagenomics of trimethylamine-utilizing Archaea in the human gut microbiome. ISME J
955 [Internet]. Nature Publishing Group; 2017 [cited 2020 Nov 25];11:2059–74. Available from:
956 /pmc/articles/PMC5563959/?report=abstract

957 57. Pruesse E, Peplies J, Glöckner FO. SINA: Accurate high-throughput multiple sequence
958 alignment of ribosomal RNA genes. Bioinformatics [Internet]. Oxford Academic; 2012 [cited
959 2020 Nov 25];28:1823–9. Available from:
960 https://academic.oup.com/bioinformatics/article/28/14/1823/218226

961 58. Kumar S, Stecher G, Tamura K. MEGA7: Molecular Evolutionary Genetics Analysis
962 Version 7.0 for Bigger Datasets. Mol Biol Evol [Internet]. Mol Biol Evol; 2016 [cited 2020 Nov
963 25];33:1870–4. Available from: https://pubmed.ncbi.nlm.nih.gov/27004904/

964 59. Letunic I, Bork P. Interactive Tree Of Life (iTOL): An online tool for phylogenetic tree
965 display and annotation. Bioinformatics [Internet]. Bioinformatics; 2007 [cited 2020 Nov
966 25];23:127–8. Available from: https://pubmed.ncbi.nlm.nih.gov/17050570/

967 60. Million M, Raoult D. Linking gut redox to human microbiome. Hum Microbiome J [Internet].
968 Elsevier; 2018;10:27–32. Available from: https://doi.org/10.1016/j.humic.2018.07.002

969 61. Mauerhofer L-M, Zwirtmayr S, Pappenreiter P, Bernacchi S, Seifert AH, Reischl B, et al.
970 Hyperthermophilic methanogenic archaea are high-pressure cell factories for H2/CO2
971 conversion. Commun Biol.

972 62. Borrel G, Brugère JF, Gribaldo S, Schmitz RA, Moissl-Eichinger C. The host-associated
973 archaeome [Internet]. Nat. Rev. Microbiol. Nature Research; 2020 [cited 2020 Nov 25]. p.
974 622–36. Available from: https://pubmed.ncbi.nlm.nih.gov/32690877/

975 63. Lyu Z, Lu Y. Metabolic shift at the class level sheds light on adaptation of methanogens to
976 oxidative environments. ISME J [Internet]. Nature Publishing Group; 2018 [cited 2020 Nov
977 25];12:411–23. Available from: https://img.jgi.doe.gov/cgi-bin/mer/main.cgi

978 64. Vallenet D, Labarre L, Rouy Z, Barbe V, Bocs S, Cruveiller S, et al. MaGe: A microbial
979 genome annotation system supported by synteny results. Nucleic Acids Res [Internet]. Oxford

980 Academic; 2006 [cited 2020 Nov 25];34:53–65. Available from:
981 http://www.genoscope.cns.fr/agc/mage.

982 65. Bateman A. UniProt: A worldwide hub of protein knowledge. Nucleic Acids Res [Internet].
983 Oxford University Press; 2019 [cited 2020 Nov 25];47:D506–15. Available from:
984 https://www.ebi.ac.uk/proteins/api/doc/

985 66. Lax S, Smith DP, Hampton-Marcell J, Owens SM, Handley KM, Scott NM, et al.
986 Longitudinal analysis of microbial interaction between humans and the indoor environment.
987 Science (80-) [Internet]. American Association for the Advancement of Science; 2014 [cited
988 2020 Nov 27];345:1048–52. Available from: /pmc/articles/PMC4337996/?report=abstract

989 67. Lax S, Smith D, Sangwan N, Handley K, Larsen P, Richardson M, et al. Colonization and
990 succession of hospital-associated microbiota. Sci Transl Med [Internet]. 2017;9:eaah6500.
991 Available from: https://stm.sciencemag.org/content/9/391/eaah6500

992 68. Qian J, Hospodsky D, Yamamoto N, Nazaroff WW, Peccia J. Size-resolved emission rates
993 of airborne bacteria and fungi in an occupied classroom. Indoor Air [Internet]. John Wiley &
994 Sons, Ltd; 2012 [cited 2020 Nov 25];22:339–51. Available from:
995 https://onlinelibrary.wiley.com/doi/full/10.1111/j.1600-0668.2012.00769.x

996 69. Shan Y, Wu W, Fan W, Haahtela T, Zhang G. House dust microbiome and human health
997 risks. Int Microbiol. International Microbiology; 2019;22:297–304.

998 70. Hewitt KM, Gerba CP, Maxwell SL, Kelley ST. Office space bacterial abundance and
999 diversity in three metropolitan areas. PLoS One [Internet]. PLoS One; 2012 [cited 2020 Nov
1000 25];7. Available from: https://pubmed.ncbi.nlm.nih.gov/22666400/

1001 71. Jeon YS, Chun J, Kim BS. Identification of household bacterial community and analysis of
1002 species shared with human microbiome. Curr Microbiol [Internet]. Curr Microbiol; 2013 [cited
1003 2020 Nov 25];67:557–63. Available from: https://pubmed.ncbi.nlm.nih.gov/23743600/

1004 72. Rintala H, Pitkäranta M, Toivola M, Paulin L, Nevalainen A. Diversity and seasonal
1005 dynamics of bacterial community in indoor environment. BMC Microbiol [Internet]. BMC
1006 Microbiol; 2008 [cited 2020 Nov 25];8. Available from:
1007 https://pubmed.ncbi.nlm.nih.gov/18397514/

1008 73. Adams RI, Bateman AC, Bik HM, Meadow JF. Microbiota of the indoor environment: a
1009 meta-analysis. Microbiome [Internet]. Microbiome; 2015;3:49. Available from:
1010 http://dx.doi.org/10.1186/s40168-015-0108-3

1011 74. Meadow JF, Altrichter AE, Bateman AC, Stenson J, Brown GZ, Green JL, et al. Humans
1012 differ in their personal microbial cloud. PeerJ [Internet]. PeerJ Inc.; 2015 [cited 2020 Nov
1013 25];2015. Available from: https://pubmed.ncbi.nlm.nih.gov/26417541/

1014 75. Withey Z, Goodall T, MacIntyre S, Gweon HS. Characterization of communal sink drain
1015 communities of a university campus. Environ DNA [Internet]. John Wiley & Sons, Ltd; 2021
1016 [cited 2021 Sep 13]; Available from: https://onlinelibrary.wiley.com/doi/full/10.1002/edn3.196

1017 76. Prussin AJ, Marr LC. Sources of airborne microorganisms in the built environment.
1018 Microbiome [Internet]. BioMed Central; 2015 [cited 2020 Dec 1];3:78. Available from:
1019 /pmc/articles/PMC4688924/?report=abstract

1020 77. Feazel LM, Baumgartner LK, Peterson KL, Frank DN, Harris JK, Pace NR. Opportunistic
1021 pathogens enriched in showerhead biofilms. Proc Natl Acad Sci U S A [Internet]. Proc Natl

1022 Acad Sci U S A; 2009 [cited 2020 Dec 1];106:16393–8. Available from:
1023 https://pubmed.ncbi.nlm.nih.gov/19805310/

1024 78. Mahnert A, Vaishampayan P, Probst AJ, Auerbach A, Moissl-Eichinger C, Venkateswaran
1025 K, et al. Cleanroom Maintenance Significantly Reduces Abundance but Not Diversity of Indoor
1026 Microbiomes. Gomes NC, editor. PLoS One [Internet]. Public Library of Science; 2015 [cited
1027 2020 Nov 25];10:e0134848. Available from: https://dx.plos.org/10.1371/journal.pone.0134848

1028 79. Moissl-Eichinger C, Auerbach AK, Probst AJ, Mahnert A, Tom L, Piceno Y, et al. Quo
1029 vadis? Microbial profiling revealed strong effects of cleanroom maintenance and routes of
1030 contamination in indoor environments. Sci Rep [Internet]. Nature Publishing Group; 2015
1031 [cited 2020 Nov 25];5:1–13. Available from: www.nature.com/scientificreports

1032 80. Emerson JB, Adams RI, Román CMB, Brooks B, Coil DA, Dahlhausen K, et al.
1033 Schrödinger's microbes: Tools for distinguishing the living from the dead in microbial
1034 ecosystems [Internet]. Microbiome. BioMed Central; 2017 [cited 2020 Nov 25]. p. 86. Available
1035 from: https://microbiomejournal.biomedcentral.com/articles/10.1186/s40168-017-0285-3

1036 81. Vaishampayan PA, Rabbow E, Horneck G, Venkateswaran KJ. Survival of bacillus pumilus
1037 spores for a prolonged period of time in real space conditions. Astrobiology [Internet].
1038 Astrobiology; 2012 [cited 2020 Nov 25];12:487–97. Available from:
1039 https://pubmed.ncbi.nlm.nih.gov/22680694/

1040 82. Gibbons SM. The Built Environment Is a Microbial Wasteland. mSystems. 2016;1:1–4.

1041 83. Korpela K, Costea P, Coelho LP, Kandels-Lewis S, Willemsen G, Boomsma DI, et al.
1042 Selective maternal seeding and environment shape the human gut microbiome. Genome Res.
1043 2018;28:561–8.

1044 84. Jarrell KF. Extreme Oxygen Sensitivity in Methanogenic Archaebacteria. Bioscience
1045 [Internet]. Oxford University Press (OUP); 1985 [cited 2020 Nov 25];35:298–302. Available
1046 from: https://academic.oup.com/bioscience/article-lookup/doi/10.2307/1309929

1047 85. Fetzer S, Conrad R. Effect of redox potential on methanogenesis by Methanosarcina
1048 barkeri. Arch Microbiol. 1993;160:108–13.

1049 86. Thauer RK, Kaster A-K, Goenrich M, Schick M, Hiromoto T, Shima S. Hydrogenases from
1050 Methanogenic Archaea, Nickel, a Novel Cofactor, and H 2 Storage . Annu Rev Biochem.
1051 2010;79:507–36.

1052 87. Yuan Y, Conrad R, Lu Y. Transcriptional response of methanogen mcrA genes to oxygen
1053 exposure of rice field soil. Environ Microbiol Rep. 2011;3:320–8.

1054 88. Angel R, Matthies D, Conrad R. Activation of methanogenesis in arid biological soil crusts
1055 despite the presence of oxygen. Gilbert JA, editor. PLoS One [Internet]. Public Library of
1056 Science; 2011 [cited 2020 Nov 25];6:e20453. Available from:
1057 https://dx.plos.org/10.1371/journal.pone.0020453

1058 89. Angel R, Claus P, Conrad R. Methanogenic archaea are globally ubiquitous in aerated
1059 soils and become active under wet anoxic conditions. ISME J [Internet]. Nature Publishing
1060 Group; 2012 [cited 2020 Nov 25];6:847–62. Available from:
1061 http://soils.usda.gov/technical/aids/investigations/texture/

1062 90. Ueki A, Ono K, Tsuchiya A, Ueki K. Survival of methanogens in air-dried paddy field soil
1063 and their heat tolerance. Water Sci Technol. No longer published by Elsevier; 1997. p. 517–

1064 22.

1065 91. Yuan Y, Conrad R, Lu Y. Responses of methanogenic archaeal community to oxygen
1066 exposure in rice field soil. Environ Microbiol Rep. 2009;1:347–54.

1067 92. Ma K, Lu Y. Regulation of microbial methane production and oxidation by intermittent
1068 drainage in rice field soil. FEMS Microbiol Ecol [Internet]. FEMS Microbiol Ecol; 2011 [cited
1069 2020 Nov 25];75:446–56. Available from: https://pubmed.ncbi.nlm.nih.gov/21198683/

1070 93. Wang Y, Yan Y, Thompson KN, Bae S, Accorsi EK, Zhang Y, et al. Whole microbial
1071 community viability is not quantitatively reflected by propidium monoazide sequencing
1072 approach. Microbiome [Internet]. BioMed Central Ltd; 2021 [cited 2021 Mar 18];9:17. Available
1073 from: https://microbiomejournal.biomedcentral.com/articles/10.1186/s40168-020-00961-3

1074 94. Adams RI, Lymperopoulou DS, Misztal PK, De Cassia Pessotti R, Behie SW, Tian Y, et
1075 al. Microbes and associated soluble and volatile chemicals on periodically wet household
1076 surfaces. Microbiome. Microbiome; 2017;5:128.

1077 95. Xu Y, Tandon R, Ancheta C, Arroyo P, Gilbert JA, Stephens B, et al. Quantitative profiling
1078 of built environment bacterial and fungal communities reveals dynamic material dependent
1079 growth patterns and microbial interactions. Indoor Air [Internet]. Blackwell Munksgaard; 2020
1080 [cited 2020 Dec 1]; Available from: https://pubmed.ncbi.nlm.nih.gov/32757488/

1081 96. Brusa T, Ferrari F, Canzi E. Methanogenic bacteria: Presence in foodstuffs. J Basic
1082 Microbiol [Internet]. John Wiley & Sons, Ltd; 1998 [cited 2020 Nov 25];38:79–84. Available
1083 from: https://onlinelibrary.wiley.com/doi/full/10.1002/%28SICI%291521-
1084 4028%28199805%2938%3A2%3C79%3A%3AAID-JOBM79%3E3.0.CO%3B2-J

1085 97. van de Pol JAA, van Best N, Mbakwa CA, Thijs C, Savelkoul PH, Arts ICW, et al. Gut
1086 Colonization by Methanogenic Archaea Is Associated with Organic Dairy Consumption in
1087 Children. Front Microbiol [Internet]. Frontiers Research Foundation; 2017 [cited 2020 Nov
1088 25];8:355. Available from: http://journal.frontiersin.org/article/10.3389/fmicb.2017.00355/full

1089 98. Taffner J, Bergna A, Cernava T, Berg G. Tomato-Associated Archaea Show a Cultivar-
1090 Specific Rhizosphere Effect but an Unspecific Transmission by Seeds. Phytobiomes J
1091 [Internet]. American Phytopathological Society; 2020 [cited 2020 Dec 1];4:133–41. Available
1092 from: https://apsjournals.apsnet.org/doi/10.1094/PBIOMES-01-20-0017-R

1093 99. Taffner J, Laggner O, Wolfgang A, Coyne D, Berg G. Exploring the Microbiota of East
1094 African Indigenous Leafy Greens for Plant Growth, Health, and Resilience. Front Microbiol
1095 [Internet]. 2020 [cited 2020 Dec 1];11. Available from:
1096 https://www.frontiersin.org/articles/10.3389/fmicb.2020.585690/full

1097 100. Youngblut ND, Reischer GH, Dauser S, Walzer C, Farnleitner AH, Ley RE. Environmental
1098 Microbiology and Molecular Diagnostics 166/5/3, Gumpendorfer Straße 1a. bioRxiv [Internet].
1099 Cold Spring Harbor Laboratory; 2020 [cited 2020 Nov 29];2020.11.10.376293. Available from:
1100 https://doi.org/10.1101/2020.11.10.376293

1101 101. Wolf A, Moissl-Eichinger C, Perras A, Koskinen K, Tomazic P V., Thurnher D. The
1102 salivary microbiome as an indicator of carcinogenesis in patients with oropharyngeal
1103 squamous cell carcinoma: A pilot study. Sci Rep [Internet]. Nature Publishing Group; 2017
1104 [cited 2020 Nov 29];7. Available from: https://pubmed.ncbi.nlm.nih.gov/28725009/

1105 102. Koskinen K, Reichert JL, Hoier S, Schachenreiter J, Duller S, Moissl-Eichinger C, et al.
1106 The nasal microbiome mirrors and potentially shapes olfactory function. Sci Rep [Internet].

1107 Nature Publishing Group; 2018 [cited 2020 Nov 29];8:1–11. Available from:
1108 https://pubmed.ncbi.nlm.nih.gov/29358754/

1109 103. Caporaso JG, Lauber CL, Walters WA, Berg-Lyons D, Huntley J, Fierer N, et al. Ultra-
1110 high-throughput microbial community analysis on the Illumina HiSeq and MiSeq platforms.
1111 ISME J [Internet]. Nature Publishing Group; 2012 [cited 2020 Nov 29];6:1621–4. Available
1112 from: www.nature.com/ismej

1113 104. Klindworth A, Pruesse E, Schweer T, Peplies J, Quast C, Horn M, et al. Evaluation of
1114 general 16S ribosomal RNA gene PCR primers for classical and next-generation sequencing-
1115 based diversity studies. Nucleic Acids Res [Internet]. Oxford Academic; 2013 [cited 2020 Nov
1116 29];41:e1–e1. Available from: www.mimas-project.de

1117 105. Raskin L, Stromley JM, Rittmann BE, Stahl DA. Group-specific 16S rRNA hybridization
1118 probes to describe natural communities of methanogens. Appl Environ Microbiol [Internet].
1119 American Society for Microbiology; 1994 [cited 2020 Nov 29];60:1232–40. Available from:
1120 https://pubmed.ncbi.nlm.nih.gov/7517128/

1121 106. DeLong EF. Archaea in coastal marine environments. Proc Natl Acad Sci U S A [Internet].
1122 National Academy of Sciences; 1992 [cited 2020 Nov 29];89:5685–9. Available from:
1123 https://www.pnas.org/content/89/12/5685

1124 107. Amann RI, Ludwig W, Schleifer KH. Phylogenetic identification and in situ detection of
1125 individual microbial cells without cultivation [Internet]. Microbiol. Rev. American Society for
1126 Microbiology; 1995 [cited 2020 Nov 29]. p. 143–69. Available from:
1127 /pmc/articles/PMC239358/?report=abstract

1128 108. El Fantroussi S, Verschuere L, Verstraete W, Top EM. Effect of phenylurea herbicides
1129 on soil microbial communities estimated by analysis of 16S rRNA gene fingerprints and
1130 community-level physiological profiles. Appl Environ Microbiol [Internet]. American Society for
1131 Microbiology; 1999 [cited 2020 Nov 29];65:982–8. Available from:
1132 https://pubmed.ncbi.nlm.nih.gov/10049851/

1133

1134

Figure and Table legends

Fig. 1: Distribution and relative abundance of bacterial taxa in samples from different households/bathrooms. Bar charts showing the microbial composition of non-PMA- and PMA-treated bathroom floor samples at the **(a)** phylum and **(b)** genus levels. Genera with < 2% rel. abundance are summarised in grey. Bubble plots display the 25 most abundant genera (bubble size reflects the relative abundance): **(c)** Household samples (H1–H10) are depicted individually for non-PMA and PMA treatment together with human samples (grey background) that represent reads from several body sites: nasal cavity, skin, vagina, urine, stool and oral samples. **(d)** Human samples compared to non-PMA (blue background) and PMA (red background) bathroom samples. Genera are coloured according to their taxonomic phylum, and taxa that predominantly contain strict anaerobes are marked by an asterisk.

Fig. 2: A comparison between the indoor and human microbiome. (a) Principal coordinates analysis plots based on Bray-Curtis dissimilarity and **(b)** alpha diversity indices (Shannon, left; richness, right) are depicted for all indoor samples (blue = untreated, red = PMA treated) together with representative human body site samples (green = nasal cavity, light blue = oral, yellow = skin, brown = stool, pink = urine, purple = vaginal). Significant differences are indicated by the different letters above the bars, as defined by a Mann–Whitney *U* test; $P < 0.05$, FDR adjusted (samples that share the same letter do not significantly differ). The proportion of microbes in 10 different bathrooms (H1 – H10) for **(c)** non-PMA and **(d)** PMA samples that can be explained by human body sites or are of unknown origin (grey). Each household is represented by a vertical bar, and values were fitted to 100%. **(e)** The proportion of microbes on different body sites that can be potentially explained by the bathroom microbiome; significant differences between treatments were defined by a Kruskal-Wallis test; **, $P < 0.01$; ***, $P < 0.001$. **(f)** The table shows mean values and standard deviations for (d) and (e); significant differences between treatments were defined by performing the Wilcoxon signed-rank test; NS, not significant; *, $P < 0.05$; **, $P < 0.01$.

Fig. 3 The effects of PMA treatment on prokaryotic abundance and composition. (a) Quantitative PCR analysis of untreated and PMA-treated bathroom floor samples using universal and archaeal primer pairs. **(b)** Wilcoxon signed-rank test analysis results, revealing the relative abundance of the 50 and 100 most abundant bacterial **(b)** families and **(c)** genera, respectively, that were significantly affected by PMA treatment. Strict anaerobic taxa are marked by an asterix. Sign.: FDR-adjusted Wilcoxon signed-rank test; *, $P_{adj} < 0.05$; ***, $P_{adj} < 0.01$. **(d)** The relative abundance of different phenotypes as determined through BugBase. Significances were automatically defined by Mann-Whitney *U* test in BugBase.

Fig. 4. Archaeal community composition in indoor samples. The relative abundance of archaeal taxa among 16S rRNA gene reads from bathroom floor surfaces at the **(a)** phylum and **(b)** genus levels. Bubble plot showing relative abundances of the 25 most-abundant archaeal genera found in bathroom and human samples: **(c)** Household samples (H1-H10) are depicted individually for non-PMA and PMA treatment of human samples (grey background) that represent reads from several body sites including nasal cavity, skin, vagina, urine, stool and oral samples. **(d)** Bubble plots of the 25 most-abundant archaeal genera, displayed according to their original samples. Relative abundance is reflected by the size of the bubbles. Genera are coloured according to their taxonomic phylum, and taxa that predominantly contain strict anaerobes are marked by an asterisk. Venn diagram of shared ASVs in **(e)** non-PMA indoor and **(f)** PMA indoor samples compared to nasal, oral, skin and stool samples (body sites that show the highest numbers of shared ASVs).

Fig. 5. Phylogenetic tree based on the sequences obtained from our study, NCBI and two other studies [5,56]**.** The circle indicates the origin of the sequences used to create the tree (see legend). The branches of the tree were coloured in different shades of green according to the taxa they represent.

Fig. 6. Observed growth of selected human-associated methanogens after exposure to 21% oxygen (air). Plots indicate the growth as determined by **(a)** OD_{600} measurements and

(b) methane production of the tested strains after exposure to an aerobic (red) or anaerobic (blue) environment for different periods of time ($n = 2$).

Tab. 1. Genes for O_2/reactive oxygen species elimination enzymes and their presence in genomes of human-associated methanogens [63]**. Explanation of letters in brackets: (a)** protein inferred from homology, **(b)** predicted protein, **(c)** putative, **(d)** ferritin-like, **(e)** function from experimental evidence in other organisms, **(f)** ferritin, dps family protein. Specific gene identifiers derived from MaGe microscope database [64] and UniProtKB [65] are displayed in each column when present. n.d.: not detected.

Supplementary files

Supplementary Figure 1. Sampling area of a representative bathroom floor.

Supplementary Figure 2. Analysis of indoor microbiome samples, displaying differences upon PMA treatment on bacterial phyla level. Depicted are taxa that were characteristic to nonPMA and PMA indoor samples. (A) LEfSe analysis, and (B) boxplots of significant different taxa defined by Wilcoxon signed-rank test: *, $P < 0.05$; **, $P < 0.01$.

Supplementary Figure 3. LEfSe analysis of bacterial taxa (phylum, class, order, family, genus-level) depicting differences of PMA and non-PMA indoor samples.

Supplementary Figure 4. PMA treated indoor samples show a significantly decreased relative abundance for some opportunistic pathogens.

Supplementary Figure 5. Comparison of archaeal signatures found on different human body sites (blue) and in the 10 analysed bathrooms (red) on phylum (top) level and for the 25 most

abundant genera (bottom). Only samples without PMA treatment were included. Sign.: *, $P < 0.05$; ****, $P < 0.0001$; Wilcoxon signed-rank test.

Supplementary Table 1. Metadata collected from all 10 households.

Supplementary Table 2. Primer pairs used for archaea and bacteria PCR and qPCR.

Supplementary Table 3. The PCR and qPCR conditions for the primer pairs used.

Supplementary Table 4. ASV table and data overview for indoor microbiomes.

Supplementary Table 5. Summary of additional datasets (human microbiome) used in this study. The study including the saliva samples (bacterial dataset), as well as the study on the nasal cavity (archaeal dataset) have already been published [101,102].

Supplementary Table 6. ASV table of all indoor and human samples, universal dataset.

Supplementary Table 7. List of shared taxa among different households.

Supplementary Table 8. List of most abundant bacterial genera, families and orders and the respective impact of PMA treatment on their relative abundance, analysed by Wilcoxon signed-rank test.

Supplementary Table 9. ASV table of all indoor samples, archaeal dataset.

Supplementary Table 10. ASV table of all indoor and human samples, archaeal dataset.

References in Supplementary Tables: [103–108]